1-1-2005

The oxidation of carbon monoxide and methane by nano and regular Fe2O3

Soon-Chul Kwon
Iowa State University

The oxidation of carbon monoxide and methane by nano and regular Fe_2O_3

by

Soon-Chul Kwon

A thesis submitted to the graduate faculty

in partial fulfillment of the requirements for the degree of

MASTER OF SCIENCE

Major: Civil Engineering (Environmental Engineering)

Program of Study Committee:
Maohong Fan (Co-major Professor)
Robert C. Brown (Co-major Professor)
Roy R. Gu (Co-major Professor)
J. Hans van Leeuwen (Co-major Professor)

Iowa State University

Ames, Iowa

2005

Graduate College
Iowa State University

This is to certify that the master's thesis of

Soon-Chul Kwon

has met the thesis requirements of Iowa State University

TABLE OF CONTENTS

LIST OF FIGURES vi

LIST OF TABLES viii

ACKNOWLEDGEMENTS ix

ABSTRACT x

CHAPTER 1. INTRODUCTION 1-2

CHAPTER 2. LITERATURE REVIEW 3

2.1 INTRODUCTION 3

2.2 CATALYST FUNDAMENTALS 5

2.2.1 Activity of catalyst 5

2.2.2 Oxidation procedures 7

2.2.3 Packed-bed reactor 8

2.3 IMPORTANCE OF CATALYTIC TREATMENT OF POLLUTANT GASES 10

2.3.1 Carbon monoxide 11

Sources of carbon monoxide 11

Standard or guidelines 12

Measurement methods 12

Levels in homes 13

Control measures 13

Harmful effects of carbon monoxide 13

Steps to escape from carbon monoxide exposure 14

Oxidation of carbon monoxide over various catalysts 14

2.3.2 Methane 16

Description 16

Sources of methane 17

Various uses of methane 19

Control of methane 19

Combustion of methane over various catalysts 20

2.4 IRON OXIDE AS CARBON MONOXIDE AND METHANE OXIDANT 21

2.4.1 Fe_2O_3 as a carbon monoxide oxidant 21

2.4.2 Fe_2O_3 as Methane oxidant 23

CHAPTER 3. EXPERIMENTAL SECTION 26

3.1 SELECTION OF CATALYSTS 26

3.2 EXPERIMENTAL APPARATUS 30

3.3 GENERAL PROCEDURE 33

CHAPTER 4. RESULTS AND DISCUSSIONS 35

4.1 OXIDATION OF CARBON MONOXIDE BY NANOCAT® AND Fe_2O_3-PVS 35

4.1.1 Effect of temperature 35

4.1.2 Effect of concentration 38

4.1.3 Effect of space time 40

4.2 OXIDATION OF METHANE BY NANOCAT® AND Fe_2O_3-PVS 44

4.2.1 Effect of temperature 44

4.2.2 Effect of concentration 46
4.2.3 Effect of space time 47
4.3 OXIDATION OF CARBON MONOXIDE MIXED WITH METHANE OVER NANOCAT® AND Fe_2O_3-PVS 50
4.3.1 Effect of temperature 50
4.3.2 Effect of concentration 53
4.3.3 Effect of space time 56

CHAPTER 5. CONCLUSION 58

CHAPTER 6. REFERENCES 59

LIST OF FIGURES

Figure 1.1. Catalyzed and uncatalyzed reaction energy paths for reactants converted to products. 6

Figure 1.2. Packed-bed reactor. 10

Figure 1.3.Schematic diagram of the flow reactor. 30

Figure 1.4. Experimental set-up for oxidation of CO and CH_4. 31

Figure 1.5. Tube Furnace and Gas Chromatograph used for oxidation of CO and CH_4. 32

Figure 1.6. Picture of catalyst inside quartz wool tube. 32

Figure 1.7. Flow meters and gas tanks for oxidation of CO and CH_4. 34

Figure 1.8. LAMCOM gas analyzer for measuring CO and CO_2. 34

Figure 2.1. Efficiency of CO oxidation by NANOCAT® and Fe_2O_3-PVS as a function of temperature. 36

Figure 2.2. Efficiencies of CO (a) and CH_4 oxidation (b) by NANOCAT® and Fe_2O_3-PVS during a period of 2 hours. 37

Figure 2.3. Efficiency of CO oxidation by NANOCAT® (a) and Fe_2O_3-PVS (b); insert Figures show: oxidation efficiency as a function of CO concentrations at various temperatures. 39

Figure 2.4. Efficiency of CO oxidation as a function of space time. 43

Figure 2.5. Efficiency of CH_4 oxidation by NANOCAT® and Fe_2O_3-PVS as a function of temperature. 45

Figure 2.6. Efficiency of CH_4 oxidation by NANOCAT® (a) and Fe_2O_3-PVS (b) as a function of concentrations; Insert Figures show: the effect of CH_4 concentration on oxidation efficiency at various temperatures. 48

Figure 2.7. Efficiency of CH_4 oxidation by NANOCAT® (a) and Fe_2O_3-PVS (b) as a function of space time. 49

Figure 2.8. Efficiency of mixed CO and CH_4 oxidation by NANOCAT® (a) and Fe_2O_3-PVS (b) as a function of temperature. 52

Figure 2.9. Efficiency of mixed CO and CH_4 oxidation during a period of 2 hours. 53

Figure 2.10. Efficiency of mixed CO and CH_4 oxidation by NANOCAT® (a) and Fe_2O_3-PVS (b) as a function of temperature at various concentrations; Insert Figures show: oxidation efficiency as a function of mixed gas concentration at various temperatures. 55

Figure 2.11. Efficiency of mixed CO and CH_4 oxidation as a function of Space time by NANOCAT®(a) and Fe_2O_3-PVS(b). 57

LIST OF TABLES

Table 1.1. Sources and sinks for CO 12

Table 1.2. Physiological effects of CO on human 13

Table 1.3. Sources and sinks for CH_4. 18

Table 2.1. Comparison of activation energy of various catalysts. 28

Table 2.2. Comparison of surface area of various catalysts. 29

ACKNOWLEDGEMENTS

I am very grateful to Dr. Maohong Fan for his knowledgeable input in my research, help in conducting the laboratory experiments, and help in writing of my thesis. I would also like to thank Dr. Robert Brown for his support of my graduate study, Dr. Roy R. Gu for his invaluable advice and guidance throughout my graduate school experience, and Dr. Hans van Leeuwen for his invaluable suggestions on my thesis. I also thank Dr. Chia-Line Chuang for the design of the experimental set-up, Glenn Norton for help in conducting the laboratory experiments.

I would also thank the administrative staff of Center for Sustainable Environmental Technologies and my friends, especially Youngran Jeong, shilpi Singh, Yonghui Shi, Na Li, and JeongHyub Ha for their co-operation and help throughout my research.

I express my deep appreciation to my wife, Myung-Hwa Jung who supported and encouraged me throughout graduate school.

Finally, I would like to dedicate this work to my parents, my two brothers, and my sister-in-law for making me capable enough to accomplish this work.

ABSTRACT

The catalytic performances of nano and regular Fe_2O_3 in the oxidation of methane (CH_4) and carbon monoxide (CO) singly and in combination were compared in a laboratory study. The major oxidation product is carbon dioxide (CO_2). The performance of the nanocatalyst for oxidation of CH_4 and CO was studied under variable conditions of temperature, concentration and space-time. It was demonstrated that 40 mg of Fe_2O_3 nanoparticles (NANOCAT® superfine iron oxide) was much more effective than 400mg of non-nano Fe_2O_3-PVS (Bailey-PVS Oxides) in calatalyzing the oxidation. Furthermore, in the oxidative coupling of CH_4 and CO, the efficiency of mixed gas conversion was also higher when NANOCAT® was used as the catalyst than when Fe_2O_3-PVS was used, and almost complete oxidation of the mixed gas phases was observed. These results support the hypothesis that the small particle size (3nm), high surface area (245 m^2/g), and denser surface coordination of the nanocatalyst can contribute to its better performance as a catalyst. Generally, the oxidation of CO and CH_4 increased significantly with increase in temperature. In the presence of oxygen, the reaction is zero-order on CO. The oxidation efficiency was not affected by the CO concentrations at any temperature (more than 200°C). However, lower concentrations in the gas phase contributed to higher oxidation efficiency over the entire range of temperatures. The oxidation of CH_4 is quite complicated, and has not been clearly delineated. An increase in the inlet gas flow rate caused a lower conversion rate. An examination of space time effect of CO oxidation reveals that the higher space time between carbon monoxide and NANOCAT® has little or no effect on oxidation efficiency. In contrary to CO oxidation, the CH_4 and mixed gas (CO and CH_4) oxidations were accelerated by increased space time with NANOCAT®.

CHAPTER 1. INTRODUCTION

Catalytic oxidation is known as one of the most widespread techniques for removing harmful emissions of several gas phases. Most articles have reported that various catalysts are particularly active in CO (carbon monoxide) or VOC (Volatile Organic Compound) catalytic oxidation. In recent years, many researchers have focused on the use of Nanocatalysts due to their high catalytic performance in comparison with other catalysts. This study focuses on three concerns: (i) oxidation of CO by nano and regular Fe_2O_3, (ii) oxidation of CH_4, volatile organic compound, by both catalysts, and (iii) oxidation of CO combined with CH_4 by the two catalysts. The catalytic activities of the two catalysts were then compared.

This thesis is organized into six chapters. The oxidation of CO and VOCs released from industrial facilities or occurring in nature is the objective of this research. Chapter 2 not only presents a literature review on the fundamentals of catalysis, but also discusses CO and CH_4 describing their sources, their effects on people, and the available removal techniques. In addition, the reaction mechanism of Fe_2O_3 as a CO and CH_4 oxidant is described.

Chapter 3 describes the experimental set-up for this study. It explains the properties of both catalysts and the experimental apparatus and procedures that were used to acquire information on the oxidation efficiencies of CO and CH_4.

In Chapter 4, results of the research are discussed: the oxidation of CO and CH_4 was carried out over nanoparticle Fe_2O_3 and compared with oxidation carried out using Fe_2O_3-PVS powder as the catalyst. The catalytic performance of the two catalysts on the oxidative activities of methane and carbon monoxide was studied under variable conditions of temperature, concentration, and space time.

Chapter 5 presents a general conclusion, including the results from Chapter 4. It also provides a few recommendations for future research.

Finally, Chapter 6 provides the list of the references for the study.

CHAPTER 2. LITERATURE REVIEW

2.1 INTRODUCTION

Catalysts have ling been used for removing harmful exhausts from car and stationary pollution sources. Exhausts containing VOCs, carbon monoxide (CO), nitric oxide (NO), and so on from industrial facilities and cars can be converted to harmless nonpollutants at reasonable temperatures with cost-effective systems utilizing heterogeneous catalysts. The use of the catalytic systems allows conversion of pollutants to non-pollutants at higher rates with lower energy consumption than conventional thermal oxidation, resulting in cost-effective pollution control [1]. To reduce the energy consumption, reaction temperature is required to be as low as possible. A catalyst improves the oxidation reaction rate, allowing faster reaction at a lower temperature. Thus, Catalytic oxidation can effectively cut down the cost of operation compared with that of uncatalyzed, thermal oxidation. The use of catalytic systems for pollutant abatement was virtually non-existent before 1970's, but they are now widely used for destruction of VOCs from stationary sources such as chemical processing plants, reduction of nitric oxides from power plants and stationary engines, and decomposition of ozone in high-flying aircrafts [2]. In the future, the use of catalytic agents for pollution abatement applications promises to grow at a strong pace.

Toxic pollutants have been considered an important environmental issue in the last decades. Carbon monoxide and methane will be the focus in this paper because of their importance in vehicle emissions [3]. Carbon monoxide is the most toxic substance with which we come into contact in our daily life. Carbon monoxide is a product of the incomplete combustion of fossil fuels, and its sources include leaking chimneys and furnaces; back-drafting from furnaces, gas water heaters, wood stoves, and fireplaces; gas stoves; generators and other gasoline powered equipment; automobile exhaust from attached garages; and tobacco smoke. Interruption of the normal supply of oxygen by CO poisoning puts at risk the functions of the heart, brain, and other vital functions of the body. Lethal and

serious sub-lethal effects of CO poisoning are reported frequently. Methane (CH_4), discharged by the petroleum and chemical industries, has been chosen for this study as being representative of volatile organic compounds (VOCs). Catalytic oxidation of CH_4 reduces CO [4]. The oxidation of carbon monoxide and methane by various catalysts has been investigated for many years, and they have proven to be efficiently oxidized at lower temperatures than are required for the thermal process. Thermal oxidation units burn CO and CH_4 at very high temperatures, usually in the range of 750-1000°C, whereas a catalytic oxidation unit operates at 350 and 500°C [5]. Several catalysts have shown to be highly efficient in the oxidation of CO and CH_4.

Among several catalysts, the precious metal (Pt, Pd) based, (*e.g.,* perovskite-type ($La_xAg_xMnO_3$)), and transition metal oxide based catalysts [6] have been extensively studied for the oxidation of toxic gases. The precious metal based catalysts are known to be highly active and stable and are used for vehicle exhaust gas control. However, the high cost of precious metals and their sensitivity to sulfur poisoning inspired this research to find a substitute. Various transition metal oxides and mixed metal oxides have been used for carbon monoxide and VOC oxidation. In recent years, many researchers have focused on the application of Nanocatalysts due to their high catalytic performance in comparison with many other catalysts [7-9]. Nanophase transition metal oxides with their small particle size, high surface area, and denser surface availability of unsaturated sites can improve the catalytic performance over that of non-nano catalysts [7]. Of the many carbon monoxide oxidation catalysts, Fe_2O_3 nanoparticles are especially attractive candidates in certain special applications, where the potential toxicity of other catalysts is of concern. Among nanoparticle metal oxides, the NANOCAT® superfine Fe_2O_3 (SFIO) nanoparticle with a particle size of 3 nm has been extensively used for CO oxidation. Li et al. [7] have evaluated and illustrated the high efficiency of NANOCAT® SFIO for CO oxidation and have shown it to be

considerably superior to other catalytic systems, especially to the other forms of iron oxide catalysts, in terms of activation at a given temperature and in conversion efficiency.

The oxidation mechanisms of CO with CH_4 by nanoparticle Fe_2O_3 and Fe_2O_3-PVS were investigated in this research. The catalytic activities of NANOCAT® SFIO and Fe_2O_3-PVS in the oxidation of CO and CH_4 oxidation by O_2 were investigated on a bench scale at different temperatures; different space time of CO with CH_4; and different concentrations of CO, CH_4, and O_2 in contact with the catalysts. The reactions were carried out as a function of CO and CH_4 concentrations, temperature, flow rates, and space time of CO and CH_4 with the catalysts, and monitored by using a gas chromatograph (GC) to analyze the outlet gas.

2.2 CATALYST FUNDAMENTALS

2.2.1 Activity of catalyst

A catalyst is a material that increases the rate (molecules converted by unit time) of a chemical reaction while itself not undergoing any permanent change. The adsorption of pollutants onto the catalyst provides chemical reaction shortcuts in which reactants are converted to products more rapidly than if no catalyst were present. This translates to reactions happening at lower temperatures, leading to savings in energy and reactor material. Since reaction rates are increased, the throughput of reactants and the amount of product are greatly increased, allowing the use of smaller reaction vessels.

Reactants undergoing conversion must pass through various energy barriers, called the activation energy (*E*), before the product is produced. Figure 1.1 shows the net enthalpy change against the reaction coordinate and the energy path of reactants to product. With the catalytic effect, the energy barrier, or activation energy, that controls in the transformation of reactant to product is lower.

The rate of reaction is inversely proportional to the exponential of the activation energy. This relationship is expressed through the rate constant k, as in Equations 1 and 2, where C_a and C_b represent the concentrations of the reactants at any given time and superscripts x and y denote their respective reaction orders [3]. The rate constant is related to the preexponential function k_0, which is a mechanistic term, and is proportional to the number of active sites on the catalyst. R and T are the universal gas constant and the absolute temperature, respectively [3].

$$\text{Rate} = kC_a^x C_b^y \tag{1}$$

$$k = k_0 \exp\left(-\frac{E}{RT}\right) \tag{2}$$

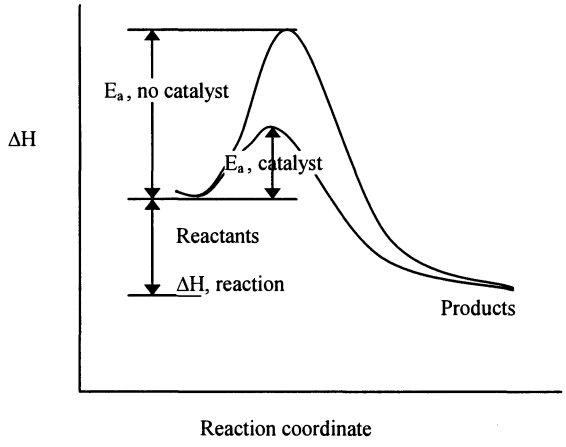

Figure 1.1 Catalyzed and uncatalyzed reaction energy paths for reactants converted to products [3].

The activation energy for the entire reaction reveals the slowest of all steps involved in converting reactant to product. The overall rate can not be greater than the slowest step. The difference between the energy states of the reactants and the products is the exothermic heat of reaction. The presence of a catalyst does not affect the enthalpy and net free energy.

Catalysts change neither the energies of the initial and final states nor the equilibrium; they affect only the rate of reaction to the final product state. Finally, catalysts enhance the kinetics of reaching equilibrium.

2.2.2 Oxidation procedures

To maximize reaction rate, it is essential to ensure accessibility of all reactants to the active catalytic sites dispersed within the internal pore network of the carrier. Here's an example of how the catalyst converts CO to CO_2:

The net reaction of CO to CO_2 is

$$CO + 0.5O_2 \rightarrow CO_2 \quad (3)$$

To convert CO to CO_2, physical and chemical steps must occur [3]:

(i) CO and O_2 contact the outer surface of the carrier containing the catalytic sites. To do so, they should diffuse through a stagnant thin layer of gas in close contact with the catalyzed carrier. Bulk molecular diffusion rates vary approximately with $T^{3/2}$ and typically have an activation energy of E_1=2-4 kcal/mol.

(ii) Since the bulk of the catalytic components are internally dispersed, the majority of the CO and O_2 molecules must diffuse through the porous network toward the active sites. The activation energy for pore diffusion, E_2, is approximately half that of a chemical reaction, or about 6-10 kcal/mol.

(iii) Once CO and O_2 molecules arrive at the catalytic site, O_2 dissociates quickly, and chemisorption of both O and CO occurs on adjacent catalytic sites. The kinetics generally follow exponential dependence on temperature, for example, $\exp(-E_3/RT)$, where E_3 is the activation energy, which for chemisorption is typically greater than 10 kcal/mol.

(iv) An activated complex forms between adsorbed CO and adsorbed O, with an energy equal to that at the peak of the activation energy profile, since this is the rate-limiting step. At

this point the activated complex has sufficient energy to convert to adsorbed CO_2. Kinetics also follow exponential dependence on temperature, for instance, $\exp(-E_4/RT)$ with activation energies typically greater than 10 kcal/mol.

(v) CO_2 desorbs from the site following exponential kinetics, for example, $\exp(-E_5/RT)$ with activation energies typically greater than 10 kcal/mol.

(vi) The desorbed CO_2 diffuses through the porous network toward the outer surface with an activation energy and kinetic similar to those in step (ii).

(vii) CO_2 must diffuse through the stagnant layer and, finally, into the bulk gas. Reaction rates follow $T^{3/2}$ dependence. Activation energies are also similar to those in step (i), less than 2-4 kcal/mol.

Step (i) and (vii) represent bulk transfer, which is a function of the specific molecules, the dynamics of the flow conditions, and the geometric surface area of the catalyst or carriers. Pore diffusion, illustrated in steps (ii) and (vi), depends primarily on the size and shape of both the pore and the diffusing reactants and product. Steps (iii), (iv), and (v) are related to the chemical interactions of reactants and products (CO, O_2, and CO_2, respectively) at the catalytic sites.

2.2.3 Packed-bed reactor

The simplest flow one could think of is plug flow: constant velocity of flow in every part of a system with no mixing between elements. Amazingly, such a simple flow is a fair approximation to actual flow in a simple channel or pipe [3]. The plug flow reactor (PFR) is used very often to study such important processes as thermal and plasma chemical reactions in the fast gas flows, catalysis area. The characteristic of a packed-bed reactor (PBR) is that material flows through the reactor as a plug. The packed-bed reactor, packed with solid catalyst particles, allows pollutants to be converted to non-pollutants by being absorbed on the catalyst surface. Packed-bed reactor advantages compared with other reactors include [3]

(i) high conversion per unit mass of catalyst, (ii) low operating cost, and (iii) continuous operation.

The principal difference between reactor design calculations involving homogeneous reactions and those involving fluid-solid heterogeneous reactions is that for the latter, the reaction rate is based on the mass of a solid catalyst, W, rather than on reactor volume, V. For a fluid-solid heterogenous system, the rate of reaction of a substance A is defined as [10]

$$-r_A' = \text{g mol A reacted/s} \cdot \text{g catalyst} \tag{4}$$

The mass of the solid is used because the amount of the catalyst is what is important to the rate of reaction; the reactor volume that contains the catalyst is of secondary significance. The design Equation was developed based on reactor volume [10]. The derivation of the design Equation for a packed-bed reactor is carried out in a manner analogous that used in the development of the tubular design Equation. To accomplish this derivation, the volume coordinate in Equation 5 for a tubular reactor is simply replaced with the catalyst weight coordinate W in Figure 1.2. As with the PFR, the PBR is assumed to have no radical gradients in concentration, temperature, or reaction rate. The Generalized mole balance on species A over catalyst weight ΔW results in the following equation [10]:

$$\text{in} \quad - \quad \text{out} \quad + \text{ generation} = \text{accumulation}$$

$$F_j(y) - F_j(y+\Delta y) + r_j \Delta V = 0 \tag{5}$$

$$F_A - F_A(W+\Delta W) + r_A' \Delta W = 0 \tag{6}$$

The dimensions of the generation term in Equation (6) are [10]

$$r_A' \Delta W \equiv \frac{\text{mole} A}{(\text{time})(\text{mass of catalyst})} \cdot (\text{mass of catalyst}) \equiv \frac{\text{mole} A}{\text{time}} \tag{7}$$

Which are, as expected, the same dimension of the molar flow rate F_A. After dividing by ΔW and taking the limit as $\Delta W \rightarrow 0$, we arrive at the differential form of the mole balance for a packed-bed reactor:

$$\frac{dF_A}{dW} = r_A' \tag{8}$$

When pressure drop through the reactor and catalyst decay are neglected, the integral form of the packed catalyst-bed design, Equation 9, can be used to calculate the catalyst weight.

$$W = \int_{F_{Ao}}^{F_A} \frac{dF_A}{r_A'} \tag{9}$$

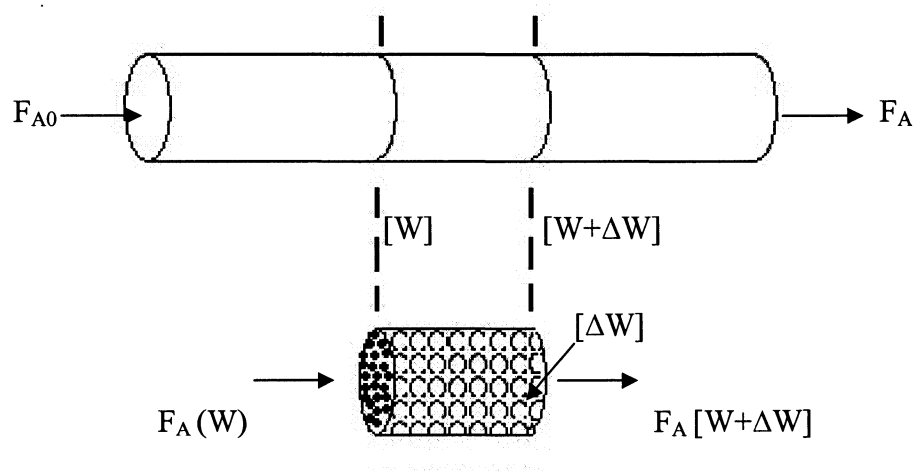

Figure 1.2 Packed-bed reactor [10].

2.3 IMPORTANCE OF CATALYTIC TREATMENT OF POLLUTANT GASES

There are a few concerns with the inlet gas phases for this study. The following sections briefly discuss CO and CH_4, in relation to their sources, their effects on people, and the removal methods used for their monitoring and abatement.

2.3.1 Carbon monoxide

Carbon monoxide (CO) is another carbonaceous gas in the earth's atmosphere that participates in the global carbon cycle. Carbon monoxide is a colorless, odorless, and tasteless gas and it burns with a violet flame. It can be slightly soluble in water and is soluble in alcohol and benzene. Carbon monoxide has a specific gravity of 0.96716, a boiling point of 190°C, a solidification point of 207 °C, and a specific volume of 13.8 ft^3/lb at 21°C. Its auto ignition temperature (liquid) is 609°C [11]. Carbon monoxide is classed as an inorganic compound.

Sources of Carbon Monoxide

Carbon Monoxide is produced by the incomplete combustion of the fossil fuels - gas, oil, coal, and wood used in boilers, engines, oil burners, gas fires, water heaters, solid fuel appliances, open fires [12], unvented kerosene and gas space heaters, leaking chimneys and furnaces, automobile exhaust from attached garages, and tobacco smoke [12]. Dangerous amounts of CO can accumulate when, as a result of poor installation, poor maintenance, or failure of or damage to an appliance in service, the fuel is not burned properly, or when rooms are poorly ventilated and the CO is unable to escape. Table 1.2 lists the sources and sinks for CO in Tg (1012 g) per year. Fossil fuel combustion is a significant source, as is biomass burning. Carbon monoxide also can be produced in secondary oxidation reactions with methane or non-methane hydrocarbons (NMHC). Major sinks include reaction with the hydroxyl radical and soil uptake. These estimates carry large uncertainties, but it is very likely that anthropogenic sources dominate natural sources. Carbon monoxide is much more reactive than carbon dioxide, so its lifetime in the atmosphere is shorter.

Standards or guidelines

No indoor air quality standards for CO have been announced [13]. The U.S. National Ambient Air Quality Standards for outdoor air are 9 ppm (40,000 μ/m^3) for 8 hours, and 35 ppm for 1 hour.

Table1.1 Sources of carbon monoxide [14]

Sources and sinks		Amount, Tg/yr
Primary Sources	Fossil Fuel	400-1000
	Biomass Burning	335-1400
	Plants	50-200
	Oceans	20-80
Secondary Sources	NMHC Oxidation	300-1400
	Methane Oxidation	400-1000
Sinks	OH reaction	2200
	Soil Uptake	250
	Stratospheric loss	100

Measurement methods [13]

Some relatively high cost infrared radiation adsorption and electrochemical instruments do exist, and moderately priced real-time measuring devices are also available. A passive monitor is currently under development, and many manufacturers have developed CO detectors that can be used in the home.

Levels in homes [13]

Average levels of carbon monoxide in homes without gas stoves vary from 0.5 to 5 ppm. Levels near properly adjusted gas stoves are often 5-15 ppm, and those near poorly adjusted stoves may be 30 ppm or higher.

Control measures [13]

It is important to be sure that combustion equipment is maintained and properly adjusted. Vehicular use should be carefully managed adjacent to buildings and in vocational programs. Additional ventilation can be used as a temporary measure when high levels of CO are expected for short periods of time.

Harmful effects of carbon monoxide

The initial symptoms of CO poisoning are similar to the flu without the fever. They include headache, fatigue, dizziness, nausea and shortness of breath. Many people with CO poisoning may mistake their symptoms for the flu or be misdiagnosed by physicians, which sometimes results in tragic deaths [13]. Table 2 shows the physiological effects produced in humans at specific levels of CO exposure.

Table 1.2 Physiological effects on human as increase in the concentration of CO [12]

Concentration of CO in air, ppm	Inhalation time and toxic developed
50	Safety level as specified by the Health and Safety Executive
200	Slight headache within 2-3 hours
400	Frontal headache within 1-2 hours, becoming widespread in 3 hours
800	Dizziness, nausea, convulsions within 45 minutes, insensible in 2 hours

Carbon Monoxide poisons by entering the lungs via the normal breathing mechanism and displacing oxygen from the bloodstream. Acute effects are due to the formation in the blood of carboxyhemoglobin, which inhibits oxygen intake [11]. Interruption of the normal supply of oxygen puts the functions of the heart, brain, and other vital functions of the body at risk. The information in Table 1.3 is for a healthy adult. Persons suffering from heart or respiratory health problems, infants and small children, unborn children, expectant mothers, and pets can be affected by CO poisoning more quickly than others in the household and may be the first to show symptoms. Moreover, CO exposure at higher concentrations can be fatal even to adults.

Steps to escape from carbon monoxide *exposure*

EPA provides several steps to reduce exposure to CO [13]: (i) keep gas appliances properly adjusted. (ii) Consider purchasing a vented space heater when replacing an unvented one. (iii) Use proper fuel in kerosene space heaters. (iv) Install and use an exhaust fan vented to the outdoors over gas stoves. (v) Open flues when fireplaces are in use. (vi) Choose properly sized wood stoves that are certified to meet EPA emission standards. Make certain that doors on all wood stoves fit tightly. (vii) Have a trained professional inspect, clean, and tune-up central heating system (furnaces, flues, and chimneys) annually and repair any leaks promptly. (viii) Do not idle the car inside garage.

Oxidation of carbon monoxide over various catalysts

Many researchers have studied CO removal in the last decades. A literature review of some of research CO oxidation is summarized below.

Li et al. [7] have studied oxidation of CO with nanoparticles of Fe_2O_3. NANOCAT® superfine Fe_2O_3 (SFIO) nanoparticles were evaluated both as a catalyst and as an oxidant for CO oxidation. The results indicate that the nanoparticles are much more effective as a CO

catalyst than the non-nano oxide powder. Experiments were carried out using a quartz flow tube reactor. The inlet gases were controlled by a flow meter, and the effluent gas was analyzed either by an NLT2000 multi-gas analyzer or a Balzer Thermal Star quadrupole mass spectrometer through a sampling procedure. During the oxidation process, the reduced form of NANOCAT® catalyzed the disproportionation reaction of CO, producing carbon deposits, iron carbide, and CO_2. For NANOCAT®, the reaction order is first-order with respect to the partial pressure of carbon monoxide, and zero-order with respect to the partial pressure of oxygen. In the absence of oxygen, NANOCAT® oxidizes CO directly as an oxidant. The higher activity of Fe_2O_3 nanoparticles over regular Fe_2O_3 was attributed to small particle size (3 nm), high surface area ($245m^2/g$), and the presence of a hydroxylated phase of iron oxide (FeOOH), as revealed by both high resolution transmission electron microscopy (HRTEM) and a comparable study of FeOOH (goethite) powder. The disproportionation reaction of CO contributes significantly to the total removal of CO.

Kang et al. [15] investigated the catalytic oxidation of CO by CoO_x/CeO_2. CoO_x/CeO_2 composite catalysts of different Co/Ce ratios have been used for CO oxidation in mixtures of CO and O_2. Composite oxides containing cobalt (Co) and cerium (Ce) catalysts were prepared by the coprecipitation method. For comparison, 10 wt.% CuO/CeO_2 composite catalysts were prepared by the procedure described above and 10 wt.% CoO_x/TiO_2 composite catalysts were prepared by the impregnation method. The catalysts were investigated by X-ray diffraction (XRD), temperature-programmed reduction (TPR), Temperature-Programmed Desorption (TPD), and X-ray Photoelectron Spectroscopy (XPS). The CoO_x/CeO_2 composite catalyst showed good resistance to water vapor poisoning, but Experiments show that CO_2 retention contributes to a fairly small but observed activity decay rate. The CoO_x/CeO_2 composite catalysts reveal high catalytic activity in CO oxidation. From the XRD, TPR and XPS results, Kang et al. [15] propose that the finely dispersed and higher valence state CoO_x species contribute to the catalytic activity.

Zhang et al. [16] made a fixed-bed reactor for studying the catalytic oxidation of CO over activated carbon (Cu/Cr/Ag/Carbon) impregnated with poly-metals (copper, chromium, and silver) as a catalyst. The conversion factor for CO was measured under different operation conditions such as reactor bed height (2 cm), catalyst particle diameter, and temperature. Once reaction starts, the oxidation on the catalyst surface increased gradually, and the oxidation of CO showed a first-order catalytic reaction.

2.3.2 Methane

Methane (CH_4), the simplest hydrocarbon, is an atmospheric constituent of which the concentration has increased in recent years. As a greenhouse gas, CH_4 is about 20 times more effective in trapping heat in the atmosphere than carbon dioxide (CO_2) over a 100-year period [17], and it is emitted from a variety of natural and human-influenced sources.

Methane is also a primary source of natural gas and an important energy source. As a result, the prevention or utilization of CH_4 emission can contribute significant energy, economic and environmental benefits. In the United States, many companies are working to reduce emissions by implementing cost-effective management methods and technologies.

Description

Methane (CH_4) is a colorless, odorless gas with a wide distribution in nature. It is the principal component of natural gas, which contains about 75% CH_4, 15% ethane (C_2H_6), and 5% other hydrocarbons, such as propane (C_3H_8) and butane (C_4H_{10}). Anaerobic bacterial decomposition of plant and animal matter, such as that which occurs under water, produces marsh gas, which is also CH_4.

At room temperature, CH_4 gas is less dense than air. It melts at –183°C and boils at –164°C. It is not very soluble in water. Methane is combustible, and mixtures of about 5-15 % in air are explosive. Methane is not toxic when inhaled, but it can produce suffocation by

reducing the concentration of oxygen inhaled. An undetected gas leak could result in an explosion or asphyxiation.

Sources of methane

Emissions from natural sources are largely determined by environmental variables such as temperature and precipitation. Even if large uncertainty remains as to the actual contributions of these natural sources, available data indicates that global methane emissions from natural sources are around 190 Tg/yr [17]. The 1992 Report of the Intergovernmental Panel on Climate Change (IPCC) lists the largest natural source of methane to be wetlands, which produce 115 Tg of carbon annually, as shown in Table 1.6. Termites are also very significant producers of methane: they eat wood and release CH_4 in the digestion process. The ocean produces about 10 Tg/yr of CH_4, and fresh water and methane hydrate contribute smaller amounts. The source of CH_4 from oceans is not clearly defined, but two identified sources are the anaerobic digestion in marine zooplankton and fish, and methanogenisis in sediments and drainage areas along coastal regions. The CH_4 emissions from methane hydrate are estimated to be around up to 5 Tg/yr from natural sources. Methane hydrates are solid deposits composed of cages of water molecules that contain molecules of CH_4. From human related sources, the largest CH_4 emissions come from the decomposition of wastes in landfills, ruminant digestion and manure management associated with domestic livestock; natural gas; and oil systems, and coal mining. Methane is the primary component of natural gas. Methane trapped in coal deposits and in the surrounding strata is released during normal mining operations in both underground and surface mines. Methane losses also occur during the production, processing, storage, transmission, and distribution of natural gas.

Table 1.3 Sources of methane [14]

Sources and sinks		Amount,Tg/yr
Natural sources	Wetlands	100-200
	Termites	10-50
	Oceans	5-20
	Freshwater	1-25
	CH4 Hydrate	0-5
Anthropogenic sources	Coal Mining, Natural gas and pet Industry	70-120
	Rice Paddles	20-150
	Enteric Fermentation	65-100
	Animal Wastes	20-30
	Landfills	20-70
	Biomass burning	20-80
Sinks	Atmospheric removal	420-520
	Removal by soils	15-45
	Atmospheric increase	28-37

Among domesticated livestock, ruminant animals (cattle, buffalo, sheep, goats, and camels) also produce significant amounts of CH_4 as part of their normal digestive processes. Methane is generated in landfills and open dumps as waste decomposes under anaerobic (without oxygen) conditions [17]. Methane is also produced during the anaerobic decomposition of organic material in livestock manure management systems.

Methane is removed from the atmosphere (i.e., converted to less harmful products) by a range of chemical and biological processes, which occur in different regions of the atmosphere and in thesoil. These include tropospheric, stratospheric oxidation and uptake by soils.

Methane can be produced in the laboratory by heating sodium acetate with sodium hydroxide and by the reaction of aluminum carbide (Al_4C_3) with water [17]. Methane is

synthesized commercially by heating a mixture of carbon and hydrogen and by the distillation of bituminous coal which contains more than 15% volatile material and by heating a mixture of carbon and hydrogen. Coal is a combustible rock, containing significant amounts of carbon, formed from the remains of decayed vegetation. Coal also contains hydrogen and oxygen, with small concentrations of nitrogen, chlorine, sulfur, and several metals. The non-volatile component of coal, which remains after distillation, is coke. Coke is almost pure carbon and is an excellent fuel. However, it may contain metals, such as arsenic and lead, which can be serious pollutants if the combustion products are released into the atmosphere.

Various uses of methane

The principal use of CH_4 is as a fuel. The combustion of CH_4 is highly exothermic. The energy released by the combustion of CH_4, in the form of natural gas, is used directly to heat homes and commercial buildings. It is also used in the generation of electric power. During the past decade natural gas accounted for about one-fifth of the total energy consumption worldwide, and about one-third in the United States [17].

In the chemical industry, CH_4 is a raw material for the manufacture of methanol (CH_3OH), formaldehyde (CH_2O), nitromethane (CH_3NO_2), chloroform (CH_3Cl), carbon tetrachloride (CCl_4), and some freons (compounds containing carbon and fluorine, and perhaps chlorine and hydrogen) [18]. The reactions of methane with chlorine and fluorine are triggered by light. When exposed to bright visible light, mixtures of methane with chlorine or fluorine react explosively.

Control of methane

Controlling emissions of CH_4 gas can reduce both air pollution and global warming, according to a new study by scientists at Harvard University, the Argonne National

Laboratory, and the EPA. They say that methane is directly linked to the production of ozone in the troposphere, the lowest part of Earth's atmosphere, extending from the surface to around 12 km (7 miles) altitude [19]. Ozone is the primary constituent of smog, and both methane and ozone are significant greenhouse gases. Ozone is formed in the troposphere by chemical reactions involving methane, other organic compounds, and CO, in the presence of nitrogen oxides and sunlight. Methane is known to be a major source of ozone throughout the troposphere, but is not usually considered to play a key role in the production of ozone smog in surface air, because of its long lifetime [19]. Reductions in methane emissions, however, would contribute decreasing greenhouse warming by decreasing both methane and ozone in the atmosphere world-wide, and this would also help to reduce surface air pollution. CH_4 can be removed by sink processes. As shown in Table 1.3, CH_4 concentration in the atmosphere determines by the balance between CH_4 emissions and methane sinks (atmospheric removal and removal by soil). Stratospheric oxidation plays a key role in atmospheric removal from the atmosphere and absorption by soil plays also a minor role in removing methane.

Combustion of methane over various catalysts

As mentioned above, combustion of CH_4 with several catalysts is known as one of best methods for removing it; some literature reviews for methane removal are provided below.

Paredes et al. [20] attempted the catalytic combustion of methane by three iron-based catalysts, prepared from waste materials from the aluminum industry (red mud (RM)) by dissolution–precipitation methods, followed by calcination. Combustion experiments were performed in a continuous packed-bed reactor, with 2mg of catalyst placed in the middle part of the reactor. The activity and stability of three iron-based catalysts for the catalytic combustion of methane were studied at atmospheric pressure, temperatures and space time, and compared with the activity and stability of hematite and a Cu-Cr-Ti commercial catalyst.

Superficial characterisation of fresh and used catalysts was carried out by BET (Brunauer, Emmett and Teller), X-ray diffraction (XRD) and temperature-programmed techniques. Experimental results indicate that red mud activated by the method of Pratt and Christoverson exhibits higher catalytic activity than the commercial catalyst and good thermal stability.

Lee et al. [21] reviewed the catalytic combustion of methane in terms of the Palladium (Pd) based catalysts, the kinetics and mechanism, deactivation of the catalyst, and mass and heat transfer in the system to form carbon dioxide and water, and then compared the catalytic performances of Pd-based catalyst with that of Platinum (Pt) supported metal oxides. They demonstrated that Pd supported on various metal oxides such as Al_2O_3 and SiO_2 has been found to be a significantly efficient catalyst. The catalytic oxidation was dependent on several factors, including the oxygen:methane feed ratio, the loading of precious metal (Pd and Pt) on the support, the nature of the support, the particle size of the precious metal, and the extent and nature of catalyst pretreatment. The reaction rate is found to be dependent on CH_4 concentration, generally to the first order or less. Because of overheating as a result of high conversions of CH_4, chemical kinetics is often affected by mass and heat transfer. Heat and mass transfer are also important factors in the later stage of the combustion process. Sintering and the thermal stability of the catalyst were dependent on the supports, and the sintering of supports and catalysts is accelerated at higher temperatures. Sulfur poisoning are the major factors causing deactivation. Sulfur oxides deactivate most noble metal catalysts with the exception of platinum.

2.4 IRON OXIDE (Fe_2O_3) AS CARBON MONOXIDE AND METHANE OXIDANT

2.4.1 Iron oxide (Fe_2O_3) as carbon monoxide oxidant

The oxidation of carbon monoxide by metal oxides can be illustrated as follows:

$$MO + CO \rightarrow M + CO_2 \quad (10)$$

$$M + 0.5O_2 \rightarrow MO \quad (11)$$

where MO represents the metal oxide used as a catalyst in this study.

In the first step, one oxygen atom from the catalyst molecule transfers to CO to form CO_2. This is an important step in determining the activity of a catalyst. Below 110 °C, the adsorption of both CO and O_2 on the nanocatalyst, Fe_2O_3, is very low, but gradually increases with increasing temperature. Likewise, CO oxidation accelerates. That is, low adsorption of CO and O_2 on Fe_2O_3 at lower temperature (<110 °C) generates low production of CO_2. The catalyst helps break of the covalent O-O bond to facilitate CO oxidation and charge rearrangement to form CO_2 from CO and dissociated oxygen atoms. Reddy et al. [22] reported that the binding energy of CO, O_2, and CO_2 are 11.23, 5.23, and 17.08 eV, respectively. Therefore, from the energy point of view, the reaction of CO with O_2 is likely to occur, but it requires a charge rearrangement to facilitate breaking of the O-O bond. The existence of the charged sites on the catalyst surface would assure the continuity of the oxidation as the adsorbed O_2 atoms at the charged sites would form charged molecules, therefore, weaken the O-O bond [22].

Fe_2O_3 catalyzes the oxidation of CO to CO_2 in the absence or presence of oxygen, with sequential reduction of Fe_2O_3 to reduced phases such as Fe_3O_4, FeO, and Fe [23]. Li et al. [7] supported the premise that in the absence of oxygen, Fe_2O_3 oxidizes CO to CO_2 with the formation of reduced phases Fe_3O_4, FeO and Fe in the sequential steps. In the presence of oxygen, however, Fe_3O_4 has been reported as the only reduced species of Fe_2O_3 in the CO to CO_2 oxidation pathways. Thus the mechanism of catalytic oxidation of CO in the presence of O_2 is simpler than that in the absence of O_2. The mechanism can be represented in the following form [24]:

$$3Fe_2O_3 + CO \rightarrow 2\,Fe_3O_4 + CO_2 \quad (12)$$

$$2Fe_3O_4 + 0.5O_2 \rightarrow 3\,Fe_2O_3 \quad (13)$$

The net reaction is

$$CO + 0.5O_2 \rightarrow CO_2 \quad (3)$$

The activity of both nano and non-nano Fe_2O_3, towards CO oxidation is dependent on reaction temperature as mentioned above. Oxidation of CO to CO_2 can be influenced by the reduction of Fe_2O_3 to Fe_3O_4 and then the intermediate Fe_3O_4 can be oxidized by O_2 to produce Fe_2O_3 again. Finally, CO oxidation with O_2 by a catalyst produced CO_2, as shown in Equation 3.

2.4.2 Iron oxide (Fe_2O_3) as methane oxidant

The oxidation of methane by metal oxides can be illustrated by the following equations:

$$4MO + CH_4 \rightarrow CO_2 + 2H_2O + 2M_2 \quad (14)$$

$$2M_2 + 2O_2 \rightarrow 4MO \quad (15)$$

where M is the metal.

The first step involves MO losing four oxygen atoms to CH_4 to facilitate the formation of CO_2 and gas phase water. To oxidize CH_4, MO as a catalyst should have the tendency of easily losing oxygen atoms due to the low reaction activity of the CH_4 molecule. At low temperatures, a very small fraction of CH_4 was adsorbed on the catalyst, so no oxidation took place. However, once adsorption of CH_4 on the catalyst surface started, the yield of CO_2 and H_2O gradually increased with increase in temperature. The increase in the reaction temperature contributes to considerable improvement of adsorption of both reactants, CH_4 and O_2.

The mechanism of catalytic oxidation of CH_4 has not been elucidated well even though it is one of the simplest hydrocarbons. The reasons are that (i) O_2 adsorption on the

catalyst surface is faster than CH_4 adsorption and (ii) the surface areas of catalysts can be covered with oxygen ahead of methane. Brown et al. assumed that the oxidation of methane could take place in different ways, depending on amount of oxygen available for the reactions, as shown below [25]:

$$CH_4 + 2O_2 \rightarrow CO_2 + 2H_2O \quad (16)$$

$$CH_4 + 1.5O_2 \rightarrow CO + 2H_2O \quad (17)$$

$$CH_4 + O_2 \rightarrow CH_3 + OH \quad (18)$$

$$CH_4 + 0.5O_2 \rightarrow CH_3OH \quad (19)$$

$$2CH_4 + 0.5O_2 \rightarrow C_2H_6 + H_2O \quad (20)$$

As shown in Equations 16-20, oxidation of CH_4 with different proportions of oxygen resulted in different products. The above reactions were formulated from observed product distributions of CH_4 oxidation for different oxygen concentrations in the inlet gas mixture [25]. An oxygen supply that is less than the maximum demand contributes to the formation of undesirable products [25]. In other words, a sufficient supply of oxygen (2moles) is needed to form harmless oxidation products, such as CO_2 and water vapor. In this study, excess oxygen was used for complete oxidation of CH_4; therefore no complicated volatile organic compounds, (*e.g.*, CH_3OH or C_2H_6) were produced.

The mechanism of CH_4 oxidation over Fe_2O_3 as a catalyst is assumed as shown below. The mechanism of Fe_2O_3 (nano and non-nano) catalyzed oxidation of $CH_4$to CO_2 takes place through a sequential reduction of Fe_2O_3, such as reduced phase Fe_3O_4 and $Fe_2O_3{\cdot}CH_4$. Methane oxidation is more complicated than CO oxidation and can be represented by the following pathways:

$$Fe_2O_3 + CH_4 \xrightarrow{k1} Fe_2O_3{\cdot}CH_4 \quad (21)$$

$$Fe_2O_3{\cdot}CH_4 + 1.5O_2 \xrightarrow{k2} CO + 2H_2O + Fe_2O_3 \quad (22)$$

$$3Fe_2O_3 + CO \xrightarrow{k3} 2Fe_3O_4 + CO_2 \quad (4)$$

$$2Fe_3O_4 + 0.5O_2 \xrightarrow{k4} 3Fe_2O_3 \quad (5)$$

The net reaction is

$$CH_4 + 2O_2 \rightarrow CO_2 + 2H_2O \quad (16)$$

Complete oxidation of CH_4 (Equation 16) can be described by Equation 21, 22, 4, and 5. In the first step, CH_4 reacts with Fe_2O_3 to produce $Fe_2O_3 \cdot CH_4$, which is then oxidized to CO, gas phase H_2O and Fe_2O_3. In the subsequent steps, CO is oxidized to CO_2 in the same fashion described earlier.

CHAPTER 3. EXPERIMENTAL SECTION

3.1 SELECTION OF CATALYSTS

The catalysts, NANOCAT® superfine Fe_2O_3 (SFIO) and Fe_2O_3-PVS, were purchased from commercial sources, March I, Inc. and Bailey-PVS Oxides, Inc. respectively, and used without any treatment. NANOCAT® SFIO is an amorphous iron oxide with a smaller particle size and greater specific area than any other forms. The product is a reddish brown, free-flowing powder with a bulk density of only 0.05 g/ml and an average particle size of 3 nm. This material has an amorphous structure and an enormous surface area of 245 m^2/g, which is much larger than that of Fe_2O_3-PVS (4 m^2/g), measured by the BET surface area test. March I, Inc., specifications indicate that the Fe_2O_3 nanoparticle not only excels as a catalyst in chemical processing with cracking and oxidation, but also provides high burning rates, has a low pressure exponent, is safe to use. Of these characteristics, the low pressure exponent, caused by a relatively low bulk density is one of the reasons for selecting this catalyst for this study. March I, Inc., provides information on the manufacture of NANOCAT® SFIO [26]. The Manufacturing process consists of diluting a gaseous, iron-containing compound with an inert carrier gas and then oxidizing this compound in a heated, oxygen-containing environment. This oxidation process yields small particles of iron oxide suspended in a heated, flowing, oxygen-containing gas stream. Then, the particle size, surface area, and morphology of the iron particulate product are modified by variations in the operation parameters. Finally, the particles that have been changed to nanometer particles are filtered and collected as a very fine free-flowing powder.

Lower activation energy (E_a) contributes to a lower onset temperature and a faster reaction. Literature values of E_a are listed in Table 2.1. NANOCAT® has the second lowest E_a value (14.5 kcal/mol) among all catalysts listed in the Table [7, 27-31]. The E_a value of Au/ Fe_2O_3, known as one of the best catalysts for CO and VOC oxidation [32-34], is larger than

that of NANOCAT®; and it is even lager than that of normal Fe_2O_3. Although the E_a value of NANOCAT® is not the lowest in the table, it contributes to a lower onset temperature and higher efficiency of CO and CH_4 oxidation than any other catalysts in the table.

The surface area of catalysts contributes to oxidation efficiency. The supports for CO and VOCs oxidation, obtained from the literature and known as the best catalysts are listed in Table 2.2 [4, 6, 30, 32, and 36-38] in the ascending order of their BET surface area. The BET surface area of NANOCAT® (245 m^2/g) is largest among all catalysts shown in the table, over 60 times larger than normal iron oxide (4 m^2/g). The larger surface area of a catalyst contributes to higher oxidation efficiency. Thus NANOCAT® has been selected as a preferred catalyst in the study. The effectiveness of nanoparticle Fe_2O_3 for methane oxidation has not been explored by other researchers, and to the best of our knowledge this is the first report on this subject.

Fe_2O_3-PVS (Physical Vapor Synthesis) was purchased from Bailey-PVS Oxides and used without further purification. Manufacturer analyses show that it consists of 99.1% of iron oxide and small amounts of other metals such as Cu, and so on. The compound is a red, a free-flowing powder with a bulk density of 0.5 g/ml, and the average particle size is 700 nm. This material has an amorphous structure and a surface area of 4 m^2/g. The main manufacturing process is the decomposition of the iron chloride solution within a spray-roasting reactor [39]. The plant consists essentially of an acid preconcentrator (also called a venturi recuperator), a spray-roasting reactor, an absorption column, and a tailgas scrubber. Spent acid from the tank farm is preconcentrated in the venturi recuperator utilizing hot gases from the reactor. The reactor consists of a cylindrical vessel that is lined with refractory ceramic material and has several burners. The chloride particles formed in the spray-roasting process produce iron oxide and hydrochloric acid gas, with the original agglomerate remaining largely intact. Hydrochloric acid gas is subsequently removed from the cooled exhaust gases in an adiabatic absorption column. Inert gases such as nitrogen, oxygen, and

carbon dioxide are then removed from the column by fan. Water is then fed into the fan and a tail gas scrubber to remove most traces of hydrochloric acid from the roaster gases.

Table 2.1 Comparison of Activation Energy (Kcal/mol) of Various Catalysts

Catalyst	E_a (kcal/mol)	Reference
2.2% Pd/ Al_2O_3	9.6	27
NANOCAT®	14.5	7
Fe_2O_3/TiO_2	19.4	28
Fe_2O_3/Al_2O_3	20	28
Au powder	20	29
Fe_2O_3	26.4	28
Au/Fe_2O_3	29	30
Gas phase	39.6	27

Table 2.2 Comparison of surface area (m^2/g) of various catalysts

Catalyst	BET Surface area (m^2/g)	Reference
Fe_2O_3-PVS	4	*
Pt/TiO_2 (W^{6+})	10	32
CuO/ZrO_2 (UFP)	16.9	6
Pt/Al2O3/Al	28.8	36
CeO_2/ $Al_{21.}O_3$	34	37
CoO_x/CeO_2	45.2	38
CuO/ZrO_2	72.8	4
Au/ Fe_2O_3	196	30
NANOCAT®	245	*

* Measured by author.

3.2 EXPERIMENTAL APPARATUS

The oxidation reactions were carried out using a quartz flow tube reactor 55 cm long and 0.9 cm in diameter. A schematic diagram of the reactor is shown in Figure 1.3.

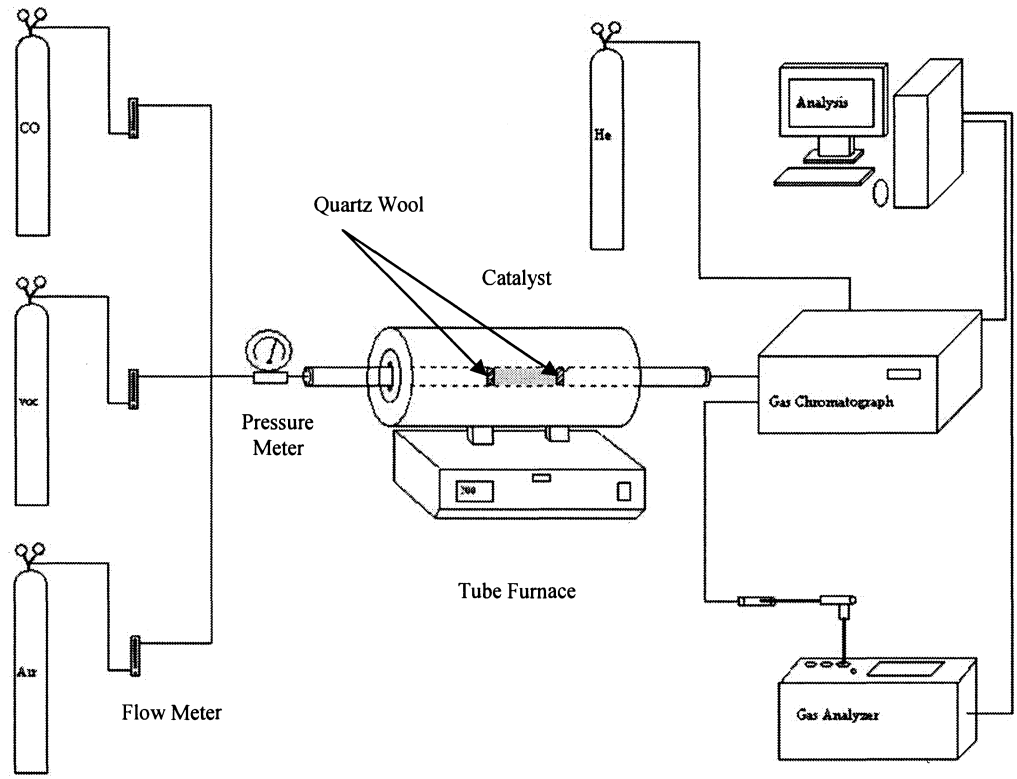

Figure 1.3. Schematic diagram of the plug-flow reactor.

Figure 1.4 also shows the real experimental set-up. The flow tube was mounted inside a Tube Furnace of type F21100 (manufactured by Barnstead/Themolyne Corporation) with a PID temperature controller as shown in Figure 1.5. The PID controller was designed to control the temperature of the reactor. The catalyst was placed in the middle of the flow tube and blocked on both sides by two pieces of quartz wool as shown in Figure 1.6. The effluent gas mixture of tube furnace was injected directly into the gas chromatograph (GC) column for analysis.

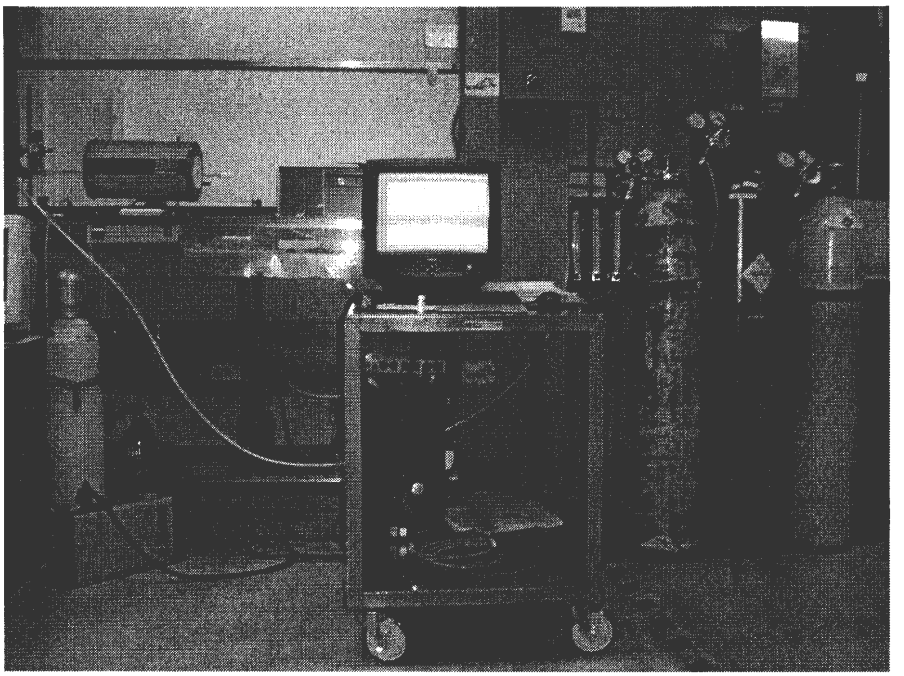

Figure 1.4. Experimental set-up for oxidation of CO and CH_4.

All experiments were performed under dry conditions using carbon monoxide or methane as an inlet gas, along with air. As shown in Figure 1.7, the flow rate of each gas was controlled accurately by the flow meter. Carbon monoxide (100%) and 10% methane in nitrogen gas were used in this study. The concentrations of methane and CO were controlled by adjusting the flow rates of these gases into an air stream. The catalyst was exposed to the mixed gas for 1 minute before any measurement. Conversion percent is the average value of three experiments using new catalysts. Over the experimental temperature range, the major product of methane oxidation was carbon dioxide, and only trace quantities of carbon monoxide (3~10ppm) were produced. Therefore, the progress of CH_4 oxidation was determined by the amount of CO_2 obtained in the effluent gas. H. Falcón et al. [4] found that carbon dioxide is the only product of CH_4 oxidation in the temperature range of 477-627°C.

Figure 1.5. Tube Furnace (left) and GC (right) for oxidation of CO and CH_4.

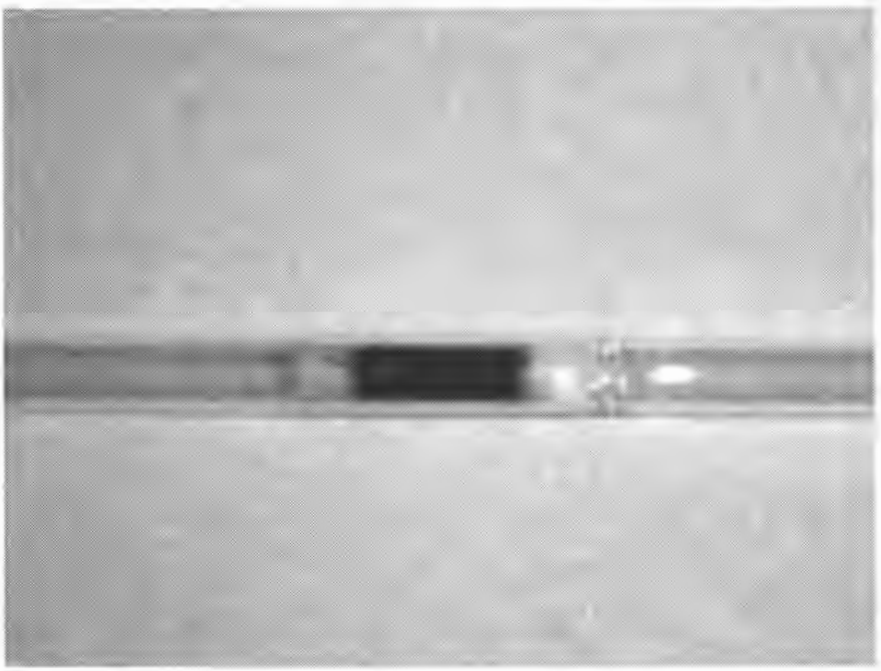

Figure 1.6. The picture of catalyst inside quartz wool tube.

3.3 GENERAL PROCEDURE

The experimental procedure included the oxidation of (i) CO with air, (ii) CH_4 with air, and (iii) CO and CH_4 with air. The effect of temperature was tested by performing the oxidation of CO over NANOCAT® at variable temperatures in the range of 100-500°C, while that of CH_4 was carried out in the range of 350-700°C. The thermal stability of NANOCAT® was tested by holding the temperature at 400°C and 700°C for CO and CH_4 oxidation, respectively. The efficiency of the catalyst may also be affected by variable concentrations of gas mixture composition. To test this effect, experiments were carried out at variable concentration ratios of inlet gas mixture by setting the flow meter to produce a variable flow rate for the inlet gases. Finally, the space time that could affect the oxidation efficiency was taken into consideration. Space time depends on the ratio of flow rate and bed volume. Because of the problem associated with adjustment of bed volume, the flow rate was changed instead. Five different flow rates were applied, while other conditions remained same. The analyses of effluent gas mixtures, to measure CO_2 as a product gas after reaction, were performed with a LAMCOM portable Flue Gas Analyzer, manufactured by LANO instruments International, as shown in Figure 1.8. Analyses of the effluent gases to measure unconverted gas were performed with a series 580 TCD gas chromatograph with a TCD (Thermal Conductivity Detector) and a stainless steel column of Carboxen-1000, manufactured by GOW-MAC, Inc., as shown in Figure 1.5. GC is a chromatographic technique that can be used to separate gases by exploiting the differences in their partitioning behavior between the mobile gas phase and the stationary phase in the column. The temperature of the column in this GC was programmed at 180°C for 30 minutes, and then the activity measurement of sample injected into GC was obtained. The GC consists of a flowing mobile phase, an injection port, a separation column containing the stationary phase, and a detector. Mobile phases-a carrier gas are generally inert gases such as helium, argon, or nitrogen. The choice of carrier gas is often dependant on the type of detector used. In the

present study, helium was used as the carrier gas. The oxidation reactions of CO and CH_4 with the Fe_2O_3-PVS catalyst were carried out under the same conditions as those used for the NANOCAT®. The efficiency of the catalyst was evaluated as a function of temperature, concentration, and space time.

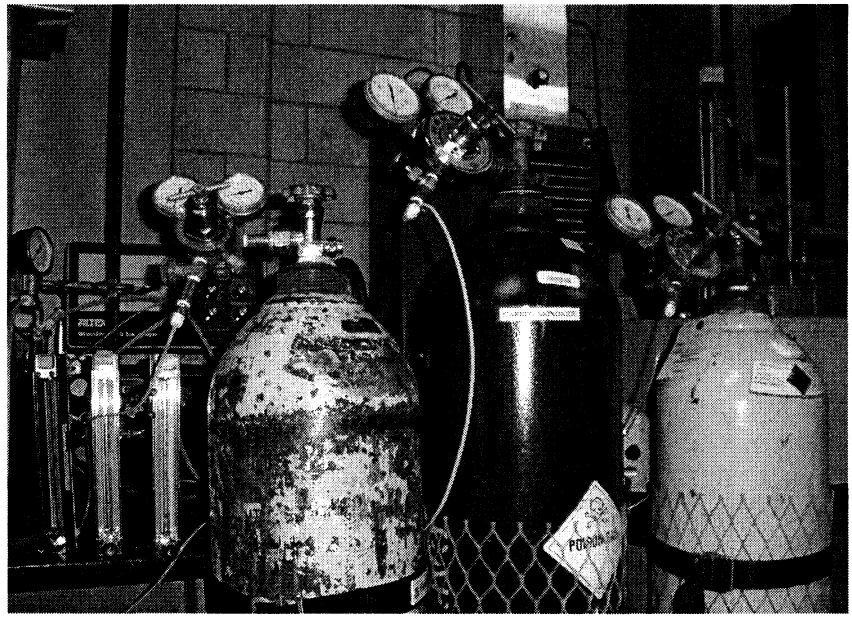

Figure 1.7. Flow meters and gas tanks for oxidation of CO and CH_4.

Figure 1.8. LAMCOM gas analyzer for measuring CO and CO_2.

CHAPTER 4. RESULTS AND DISCUSSIONS

In this study, the effectiveness of NANOCAT® and of Fe_2O_3-PVS for the oxidation of CO and CH_4 were examined and compared by monitoring the reactions at variable temperatures and concentrations of CO and CH_4. The effect of space time on the oxidation efficiency was also studied.

Oxidation efficiencies of CO and CH_4 were defined as follow:

$$\text{CO Oxidation efficiency (\%)} = \frac{[CO_2]_{Outlet}}{[CO]_{Inlet}} \times 100 \quad (23)$$

$$\text{CH}_4\text{ Oxidation efficiency (\%)} = \frac{[CO_2]_{Outlet}}{[CH_4]_{Inlet}} \times 100 \quad (24)$$

$$\text{CO+CH}_4\text{ Oxidation efficiency (\%)} = \frac{[CO_2]_{Outlet}}{([CO]_{Inlet} + [CH_4]_{Inlet})} \times 100 \quad (25)$$

Where $[CO_2]_{Outlet}$ is CO_2 concentration, the product of CO and CH_4 oxidation by catalysts (%); $[CO]_{Inlet}$ is initial concentration of CO (%); $[CH_4]_{Inlet}$ is initial concentration of CH_4 (%). The uncertainty of measurement results for collected data is ± 0.1(%).

4.1 OXIDATION OF CARBON MONOXIDE BY NANOCAT® AND Fe_2O_3-PVS

4.1.1 Effect of temperature

A preliminary reaction was carried out with 6.6% CO with air and 40 mg of NANOCAT® at a flow rate of 55 cm^3/min of inlet gas mixture over the catalysts. The result was compared with those of a reaction with 400 mg of Fe_2O_3-PVS under identical conditions. Both the 40 mg of NANOCAT® and 400 mg of Fe_2O_3-PVS were dusted onto quartz wool so that the volumes of the catalysts in the flow tube were the same. The oxidation efficiency of the catalysts was determined by analyzing the yield of CO_2 in the effluent gas mixture, as CO_2 is the major oxidation product of CO. The result, shown in Fig. 2.1, revealed that only

40 mg of NANOCAT® can completely oxidize CO to CO_2 at 400°C, whereas 400 mg of Fe_2O_3-PVS was needed for less than 65% oxidation at the same temperature. Moreover, the light off temperature where the reaction initiates with NANOCAT® SFIO is 130°C, which is lower than that for Fe_2O_3-PVS because of NANOCAT® SFIO's lower bulk density and higher surface area.

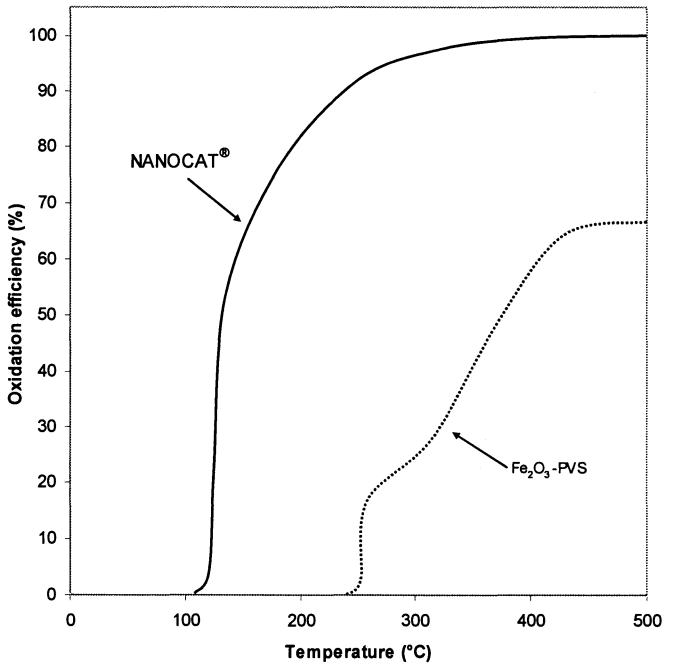

Figure 2.1. Efficiency of CO oxidation by NANOCAT® and Fe_2O_3-PVS as a function of temperature (Mass of NANOCAT®, 40mg; mass of Fe_2O_3-PVS, 400mg; flow rate of gas mixture, 55 cm^3/min; CO, 6.6%; air, 93.4%).

As demonstrated above, the NANOCAT® is more effective than Fe_2O_3-PVS. First of all, the initiation temperature is 100°C lower (130°C versus 250°C). Secondly, the CO conversion is higher with the NANOCAT®. For example, 40 mg of NANOCAT® oxidized all the CO gas (6.6% CO at a flow rate of 55 cm^3/min) to CO_2 at 400°C. Under the same experimental conditions, 400 mg of Fe_2O_3-PVS could only convert about 62 % to CO_2. Li et

al. [7] reported that 1000 mg of Fe_2O_3/TiO_2 catalyst oxidized only 10% of 2.7% CO (saturated, balanced with N_2) to CO_2 at 250°C at a flow rate of 1000 cm^3/min.

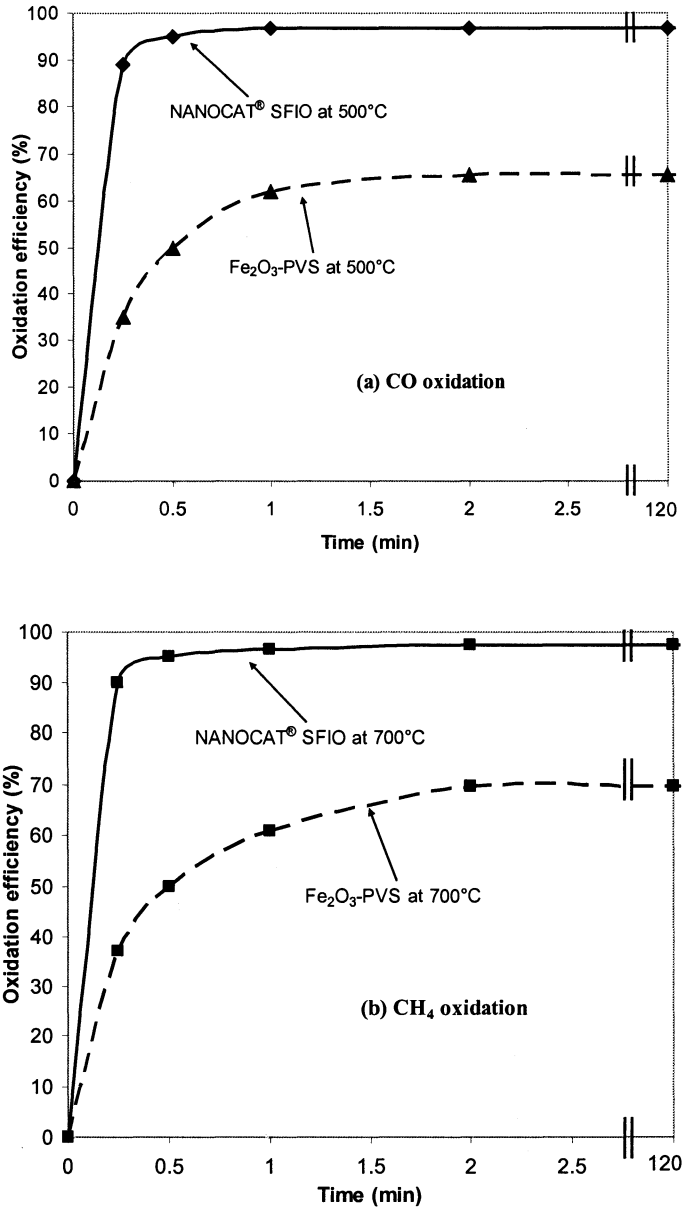

Figure 2.2. Efficiencies of CO (a) and CH_4 (b) oxidation during a period of 2 hours by NANOCAT® and Fe_2O_3-PVS (Mass of NANOCAT®, 40mg; mass of Fe_2O_3-PVS, 400mg; flow rate of gas mixture, 55 cm^3/min; CO, 6.6% at 400°C; CH_4, 1% at 700 °C; balanced with air).

In this study, the oxidation efficiency of NANOCAT® at 250°C is 94% compared with 0% for Fe_2O_3-PVS. Thus, the NANOCAT® is an efficient and beneficial catalyst for the CO oxidation process and hence can be considered one of the most economical treatment methods for CO. Long-term activity maintenance is one of the most important properties of a catalyst. To further test the stability of the NANOCAT® and Fe_2O_3-PVS, more experiments were performed holding the catalyst's temperature at 400°C as shown in Figure 2.2. 99% oxidation of CO by NANOCAT® and 61.6% conversion efficiency by Fe_2O_3-PVS was achieved in less than 1 min. And the catalytic activity of both two different types of Fe_2O_3 toward CO oxidation was stable for more than 2 hours.

4.1.2 Effect of concentration

The effect of CO concentrations on the oxidation of CO to CO_2 by NANOCAT® and Fe_2O_3-PVS is shown in Figures 2.3a and b. The temperature and CO concentrations were varied, but the total flow rate was fixed at 55 cm^3/min. The results indicated that the lower concentration of CO contributed to higher oxidation efficiency at 150 °C, followed by near almost saturation at higher temperatures. Figure 2.3a shows that the oxidation of CO by NANOCAT® reached to 95% efficiency at 300°C under 15% CO concentration compared with maximum 40% oxidation by Fe_2O_3-PVS in Figure 2.3b. The progress of the oxidation reaction appeared increase linearly in the temperature range of 150°C-200°C and revealed no significant improvement with further increasing temperatures to 350°C. Figure 2.3b reveals the gradual increase in CO oxidation efficiency to 70% by Fe_2O_3-PVS at 300-500°C. Insert Figure 2.3a indicates the reaction order of CO oxidation by NANOCAT® at different temperature. At 150 °C, the CO oxidation is inversely dependent on its concentrations. But at 200°C and beyond CO concentration has very little or no effect on the oxidation, indicating a zero-order reaction on [CO].

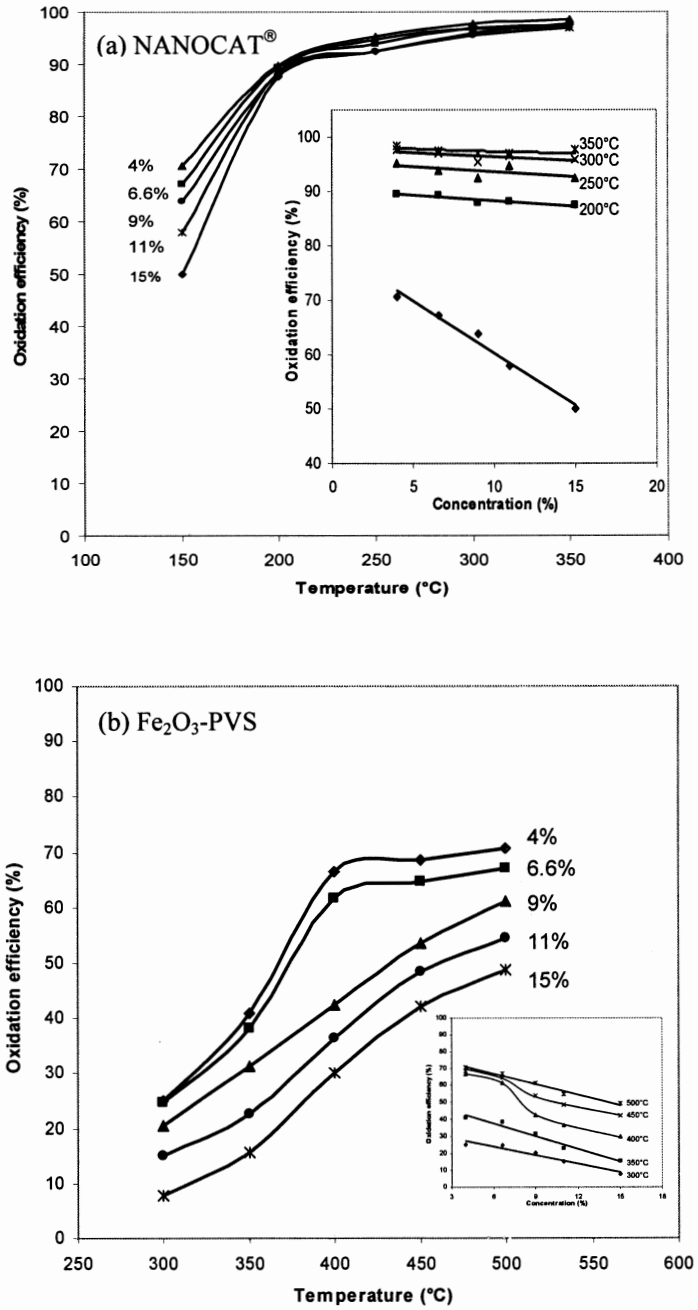

Figure 2.3. Efficiency of CO oxidation by NANOCAT® (a) and Fe_2O_3-PVS (b) at various concentrations; Insert Figures show oxidation efficiency as a function of CO concentrations at various temperatures. (Mass of NANOCAT®, 40mg; mass of Fe_2O_3-PVS, 400mg; flow rate of gas mixture, 55 cm^3/min).

Contrary to our observation, Li et al. [7] found the first-order reaction on [CO] at 244°C in the oxidation of CO by NANOCAT®, but they used a very low concentration of CO (0.5-2.1%). Walker et al. [28] also reported the first-order reaction when 2.5% of CO on 100 mesh Fe_2O_3/TiO_2 was used. Therefore, it is reasonable to suggest that the reaction follows first-order dependence on [CO] at low concentrations, but zero-order at higher concentrations of CO. Insert Figure 2.3b demonstrates the Fe_2O_3-PVS catalyzed oxidation of CO. The percentage of CO oxidation is inversely dependent on its concentrations in the range of 300-500°C. A linear decrease of CO oxidation with increasing concentrations was noted at 300, 350 and 500°C, whereas a sharp decrease was observed at 7-11% of CO at 400 and 450°C, which could be due to experimental error.

As shown in Equation (5), the net reaction of CO oxidation is

$$CO + 0.5O_2 \rightarrow CO_2 \quad (3)$$

The net reaction rate of CO oxidation by O_2 is shown below:

$$\upsilon = k\,[CO][O_2]^{0.5} \quad (26)$$

Considering the zero-order reaction on CO, Equation (26) can be written as

$$\upsilon = k\,[O_2]^{0.5} \quad (27)$$

Thus, the reaction rate of CO oxidation depends on oxygen concentrations. However, the reaction-order of the Fe_2O_3-PVS catalyzed oxidation is not clear as inverse dependence of CO oxidation on its concentrations was noted.

4.1.3 Effect of space time

For heterogeneous catalytic reactors, the term "space time" represents the average length of time that it takes a fluid element to travel from the reactor inlet to the reactor outlet [40]. Using this convention, a space time of 1min means that every 1minute one reactor volume of feed (measured at inlet conditions) is processed by the catalytic reactor. That is,

the term "space time" implies the ratio of the mass flow rate of feed to the mass of catalyst used (W).

The reciprocal of the space velocity is the space time τ as follow [40]:

Space time: $\tau = \frac{1}{WHSV} = \frac{W}{\rho Q}$ (28)

Where ρ is the mass density of the feed, Q *is volumetric flow rate of fluid* and WHSV is termed the *weight hourly space velocity.*

The space time is usually not equal to the actual residence time in the reactor. Variations in the temperature, pressure, and moles of reaction mixture can cause the local density to change through the reactor and to be unequal to the density ρ of inlet gases. Hence, there may well be a distribution of residence times in the fluid leaving, so that we must use the concept of a mean residence time. The mean residence time is equal to space time τ only when the following conditions are met [40]: (i) the temperature and pressure are constant throughout the reactor, (ii) the feed flow rate is measured at the temperature and pressure in the reactor, and (iii) the density of the reaction mixture is almost constant. Our experimental conditions satisfied these criteria, so we can evaluate the space time as a mean residence time.

Experiments were performed at five different flow rates of inlet gas mixture at a fixed CO concentration (6.6%) for both NANOCAT® and Fe_2O_3-PVS. The space time was calculated from Equation (28). The space time depends on the catalyst bed volume to flow rate ratio, and adjustment of catalyst bed volume is a difficult process. Therefore, the feed flow rate of the inlet gas mixture was varied to study this effect. The flow rate was obtained from flow meter readings. The volume of the catalyst bed was calculated from the diameter of the quartz flow tube and the length of catalysts used.

For NANOCAT® SFIO, the volume of the catalyst bed was reduced at higher temperature because the nanoparticles sintered. However, the change at low space time is not as predominant as at high space time. Peukert et al. [41] also indicated that nano-catalysts

might sinter because of their high mobility at higher temperature if the particles were not stabilized. Note that the shrinkage of NANOCAT® volume did not affect its efficiency in CO oxidation which corresponds to no change in the characteristics of the original catalyst.

The oxidation efficiency improves with decreases in the flow rate, which may be attributed to an increase in contact time between the inlet gas and the catalyst bed. Examination of Figure 2.4a reveals that the percentage of CO oxidation as a function of space time remains constant at 250, 300 and 350°C. However, at 150 and 200°C, the CO oxidation follows a bell-shaped curve as a function of space time. For Fe_2O_3-PVS catalyst (Figure 2.4b), the oxidation increases linearly against the space time up to 0.42 seconds, followed by no significant change at all temperatures. Comparison of Figures 2.4a and 2.4b reveals the following: (i) the catalytic performances of NANOCAT® and Fe_2O_3-PVS towards CO oxidation were 98% and 47%, respectively at 350 °C and the longest space time (1.1 minute and 10.3 minutes, respectively). (ii) At temperatures above 250°C, higher space time of the inlet gas has very little effect on the effectiveness of NANOCAT® catalyzed oxidation of CO, whereas the effectiveness of Fe_2O_3-PVS catalyzed oxidation gradually increases as a function of higher space time over all temperatures. These results show that NANOCAT® exhibits high catalytic activity regardless of the space time at high temperatures.

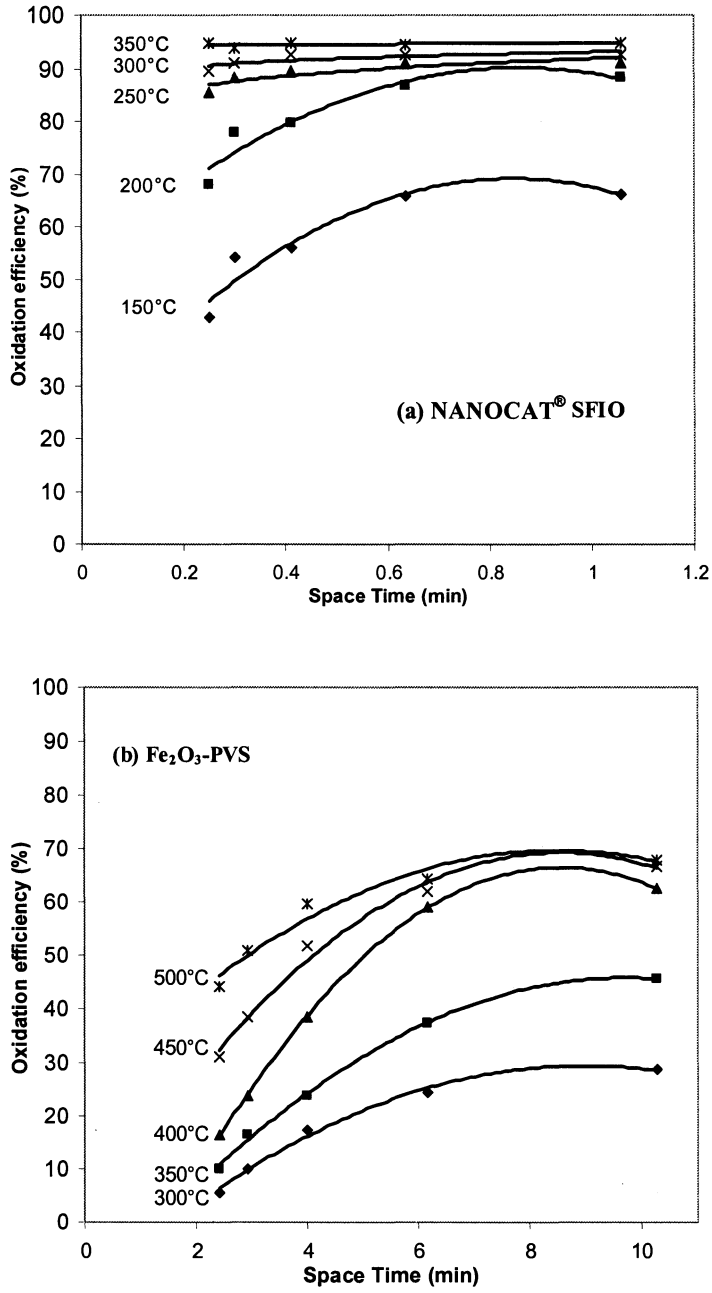

Figure 2.4. Efficiency of CO oxidation as a function of space time (Mass of NANOCAT®, 40mg (a); mass of Fe_2O_3-PVS, 400mg (b); CO, 6.6%; air, 93.4%).

4.2 OXIDATION OF METHANE BY NANOCAT® AND Fe_2O_3-PVS

4.2.1 Effect of temperature

The catalytic oxidation of CH_4 is more complicated than that of carbon monoxide. A high temperature is needed to initiate the oxidation, even in the presence of catalysts. Because of the high activation energy of methane C-H bond: the breaking C-H bond of CH_4 is more difficult than breaking the C-O bond of CO. However, once the reaction starts, subsequent steps are fast and the oxidation takes place rapidly. Moreover, the reaction produces a significant amount of heat [42]. A preliminary reaction of methane oxidation as a function of temperature is demonstrated in Figure 2.5 for both nano and non-nano catalysts. The result shows that only 40 mg of NANOCAT® can catalyze the complete oxidation of CH_4 to CO_2 in an inlet gas mixture of 1% CH_4 at 700°C and at a 55 cm^3/min of flow rate. Under the same conditions, 400 mg of Fe_2O_3 -PVS catalyst was needed for less than 70% CH_4 oxidation.

As mentioned above, the NANOCAT® is much more effective and active than other supported or non-supported iron oxide catalysts. First, the initial light off temperature (380°C) of NANOCAT® SFIO catalyzed oxidation is 90°C lower than that of Fe_2O_3-PVS (470°C). Lee et al. [*25*] observed that the light off temperature of Pd/Al_2O_3 (525°C) catalyzed CH_4 oxidation, one of the expensive novel metals based catalysts, was 145°C higher than that of NANOCAT® SFIO, and Lee et al. and Paredes et al. [25-26] also reported that a high temperature is required to activate CH_4 oxidation. Thus, the CH_4 oxidation requires a high activation temperature than CO oxidation. Secondly, the percentage of CH_4 oxidation by NANOCAT® is higher than that by other catalysts. At 470°C, where the Fe_2O_3-PVS catalyzed oxidation initiated, the NANOCAT® catalyzed oxidation of methane was already more than 60% complete.

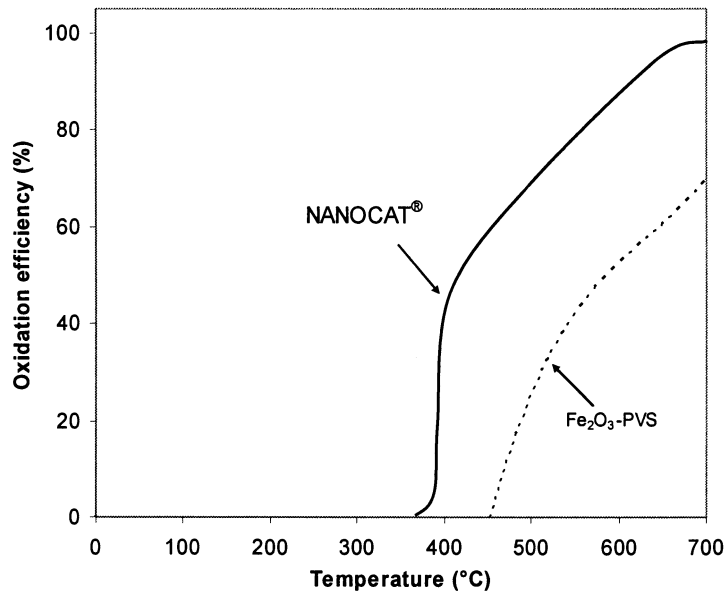

Figure 2.5. Efficiency of CH_4 oxidation by NANOCAT® and Fe_2O_3-PVS as a function of temperature (Mass of NANOCAT®, 40mg; mass of Fe_2O_3-PVS, 400mg; flow rate of gas mixture, 55 cm^3/min; CH_4, 1%; air, 99%).

Compared with other catalytic oxidations, He et al. [9] reported that 300 mg $La_2O_3/BaCO_3$ nanocatalyst with a particle size of 77 nm was inactive to CH_4 oxidation at 470°C. Lyubovsky et al. [43] demonstrated that the catalytic oxidation efficiency of Pd catalyst acting on 1% CH_4 by 15% at 470°C, and 90% at 800°C. Thus, the high oxidation efficiency of a small amount of nanocatalyst acting on CH_4 indicates that NANOCAT® is the most promising catalytic system for CH_4 oxidation.

To further test the long-term activity of the NANOCAT® and Fe_2O_3-PVS for CH_4 oxidation, experiments were carried out holding the catalyst's temperature at 700°C. A mixture of 1% CH_4 and air was used as the inlet gas. The result as shown in Figure 2.2b revealed that 98 and 70% of the CH_4 was effectively oxidized with the NANOCAT® and

Fe_2O_3-PVS catalysts, respectively, in less than 1 minute, followed by no change for more than 2 hours.

4.2.2 Effect of concentration

These reactions were performed at variable CH_4 concentrations and temperatures, but the flow rate of inlet gas was fixed at 55 cm^3/min. Figures 2.6a and 2.6b demonstrates the percentage of CH_4 oxidation as a function of its concentrations. Like CO oxidation, CH_4 oxidation was found to be most effective at lower concentrations with both NANOCAT® and Fe_2O_3-PVS catalysts. The progress of the oxidation reaction with both catalysts showed a gradual increase of CH_4 oxidation up to 98% and 70%, respectively, at our experimental temperature and at ≤ 6.6% CH_4. However, the reaction started with ≥ 8.9% methane resulted in poor oxidation efficiency even at 700°C. Insert Figure 2.6a represents the NANOCAT® catalyzed oxidation of CH_4 as a function of CH_4 concentrations. The percentage of CH_4 oxidation decreased linearly with the increase in CH_4 concentration up to 6.6%, and sharply decreased at higher concentrations. Insert Figure 2.6b shows the Fe_2O_3-PVS catalyzed oxidation of CH_4 against its concentration. The progress of oxidation followed an inverse dependence on CH_4 concentrations at all temperatures.

As shown in Equation 5, the net reaction of methane oxidation is

$$CH_4 + 2O_2 \rightarrow CO_2 + 2H_2O \qquad (16)$$

The reaction rate of methane oxidation can be written as:

$$\upsilon = k_1[Fe_2O_3][CH_4] + k_2[Fe_2O_3 \cdot CH_4][O_2]^{1.5} + k_3[Fe_2O_3]^3[CO] + k_4[Fe_3O_4]^2[O_2]^{0.5} \qquad (29)$$

The overall reaction rate (Equation 29) of CH_4 oxidation is quite complicated, and intermediate products have not been clearly identified. Absorption rates of CO and CH_4 on the catalyst surface are different. Most likely adsorption of CO on the catalyst surface is higher than that of CH_4. Therefore, as soon as CO is formed during the process of CH_4

oxidation, adsorption of CH_4 on the catalyst surface decreases. Thus, the overall rate of CH_4 oxidation decreases as adsorption of CH_4 is hindered by intermediate CO adsorption. The total reaction rate depends on individual rate constants value, $k_1 - k_4$, which have not yet been reported.

4.2.3 Effect of space time

Reactions were carried out at five different flow rates of inlet gas mixture at fixed CH_4 concentration (1%) for both NANOCAT® and Fe_2O_3-PVS catalysts, and as depicted in Figures 2.7a and 2.7b which demonstrate the percentage of CH_4 oxidation as a function of space time. The efficiency of NANOCAT® catalyzed oxidation increased with increase in space time at 450-700°C (Figure 2.7a). The effect, however, is more predominant at lower space time (< 0.6 min for NANOCAT® SFIO and < 6.1 min for Fe_2O_3-PVS), where oxidation takes place rapidly, followed by a slow oxidation at higher space times. The Fe_2O_3-PVS catalyzed oxidation of CH_4 follows a similar pattern as a function of space time, but efficiency is lower than that for NANOCAT® (Figure 2.7b). Comparison of NANOCAT® catalyzed oxidation of CO and CH_4 (Figures 2.4a and 2.7a) reveals that 98% efficiency of CO and CH_4 oxidation is achieved at 350 and 700 °C, respectively, and suggests that CO oxidation is less dependent on space time than CH_4 oxidation.

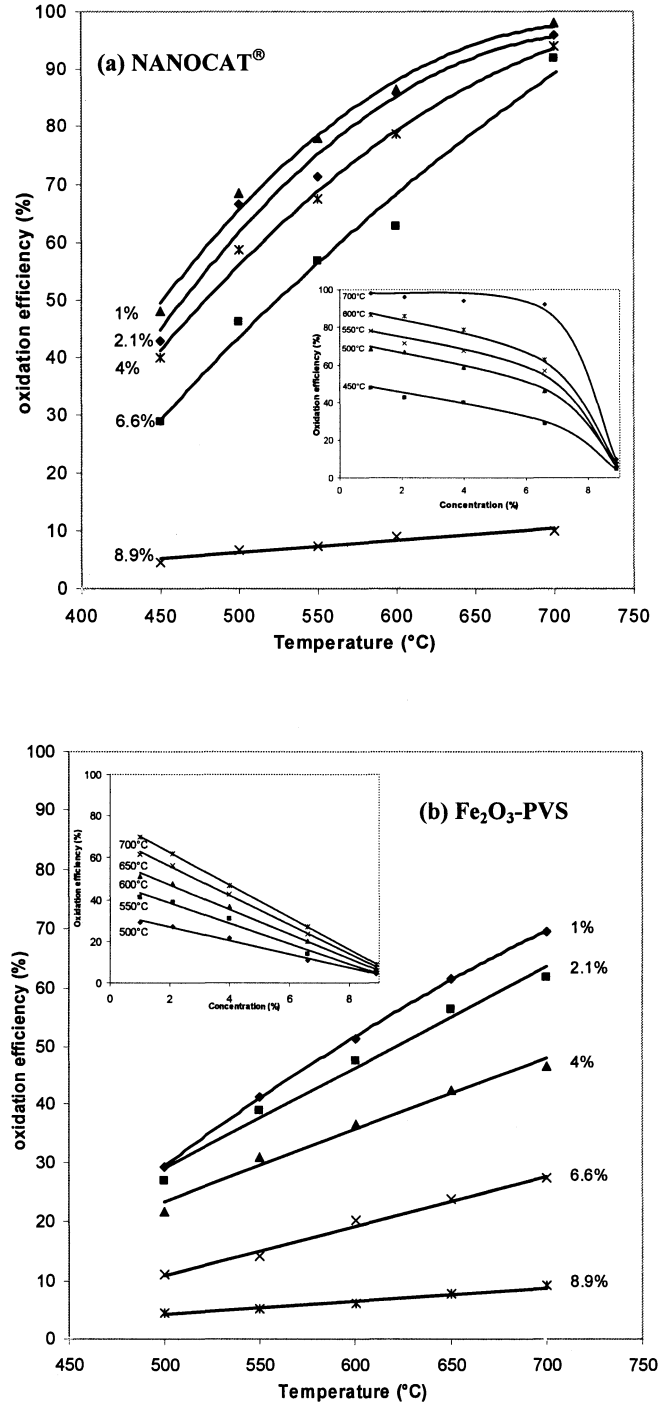

Figure 2.6. Efficiency of CH_4 oxidation by NANOCAT® (a) and Fe_2O_3-PVS (b) as a function of temperature; Insert Figures show the effect CH_4 concentration on oxidation efficiency at various temperatures (Mass of NANOCAT®, 40mg; mass of Fe_2O_3-PVS, 400mg; flow rate of gas mixture, 55 cm^3/min).

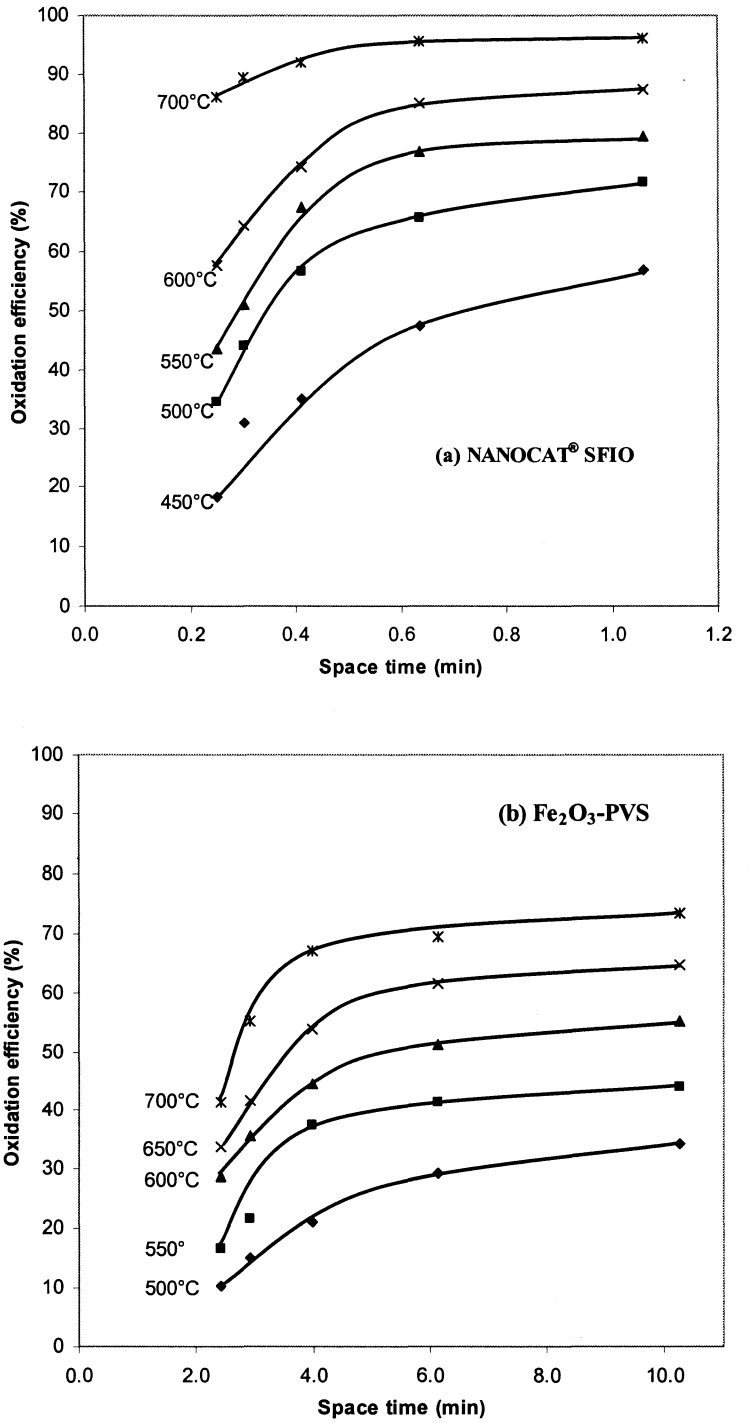

Figure 2.7. Efficiency of CH_4 oxidation as a function of space time by NANOCAT® (a) and Fe_2O_3-PVS (b) (Mass of NANOCAT®, 40mg; mass of Fe_2O_3-PVS, 400mg; CH_4: 1%; air, 99%).

4.3 OXIDATION OF CARBON MONOXIDE MIXED WITH METHANE OVER NANOCAT® AND Fe_2O_3-PVS

4.3.1 Effect of temperature

A preliminary reaction was carried out by 40 mg of NANOCAT® SFIO supplied with 6.6% CO and 1% CH_4 with air at a flow rate of 55 cm^3/min. The oxidation efficiency of the catalysts was determined by analyzing the yield of CO_2 in the effluent gas mixture. The oxidation efficiency of NANOCAT® SFIO for combined CO and CH_4 increased considerably in the temperature range of 115°C-200°C and showed slow improvement as the temperature was increased to 700°C as shown in Figure 2.8a. Figure 2.8b shows that a gradual increase in the oxidation efficiency with the Fe_2O_3-PVS catalyst was observed at 250-600°C, followed by a sharp increase from 68 to 92% in the temperature range of 550-650°C. Moreover, the initial ignition temperature (115°C) for NANOCAT® is 135°C lower than that (250°C) for Fe_2O_3-PVS because of the lower bulk density and higher surface area of NANOCAT®.

As recognized above, the NANOCAT® is more effective than Fe_2O_3-PVS in the oxidation of the combined CO and CH_4. First, the initiation temperature is 100°C lower (130°C versus 250°C), and the conversion process is faster. For example, 40 mg of NANOCAT® oxidized 98.7% of the combined CO and CH_4 to CO_2 at 500°C. Under the same experimental conditions, 400 mg of Fe_2O_3-PVS could only convert about 60.9 % of the mixed gas to CO_2. Secondly, the conversion efficiency of CO with CH_4 over NANOCAT® is higher than that of CO with CH_4 over Fe_2O_3-PVS. For example, 40 mg of NANOCAT® oxidized 86.2% of the mixed gas (6.6% CO, 1% CH_4 at 55 cm^3/min flow rate) to CO_2 at 350°C. At the same temperature, 400 mg of Fe_2O_3-PVS could only convert 22.4% of CH_4. Note that despite the use of two different types of inlet gas phases in our study the oxidation efficiency of NANOCAT® for CO mixed with CH_4 at 250°C was 82.9%, compared with 5.3% for Fe_2O_3-PVS. When compared with the CH_4 oxidation efficiency (70%) for the Fe_2O_3-PVS catalyst at 700°C, the mixed gas oxidation showed higher efficiency (94%)

because CO (6.6%), which is more easily oxidized than CH_4 (1%), is main component of the mixed gases.

Although the ration of CO in the mixed gases was higher than that of CH_4, the progress of oxidation for mixed gases was dominated by CH_4 because breaking its C-H bonds to activate the reaction is more difficult than breaking the C-O bond of CO; thus, catalytic oxidation of CH_4 is more complicated. However, once the CH_4 reaction starts, subsequent steps are fast, and the oxidation takes place rapidly. For example, at 500°C, NANOCAT® (Figure 2.8a) oxidized 100% of CO and 66.5% of CH_4 while Fe_2O_3-PVS oxidized 67.2% of CO and 30% of CH_4 as shown in Figure 2.8b. Thus, the NANOCAT® is an efficient and beneficial catalyst for the CO oxidation process and hence can apply as one of the most economical methods for treating CO and CH_4.

To further test the long-term stability of the NANOCAT® and Fe_2O_3-PVS, more experiments were carried out holding the catalyst temperature at 700°C as shown in Figure 2.9. NANOCAT® SFIO achieved 95.1% oxidation of CO mixed with CH_4 while Fe_2O_3-PVS achieved 90.9% conversion efficiency (both in less than 1.5 min). The catalytic activity of both types of Fe_2O_3 toward CO oxidation was stable at almost 98% for more than 2 hours.

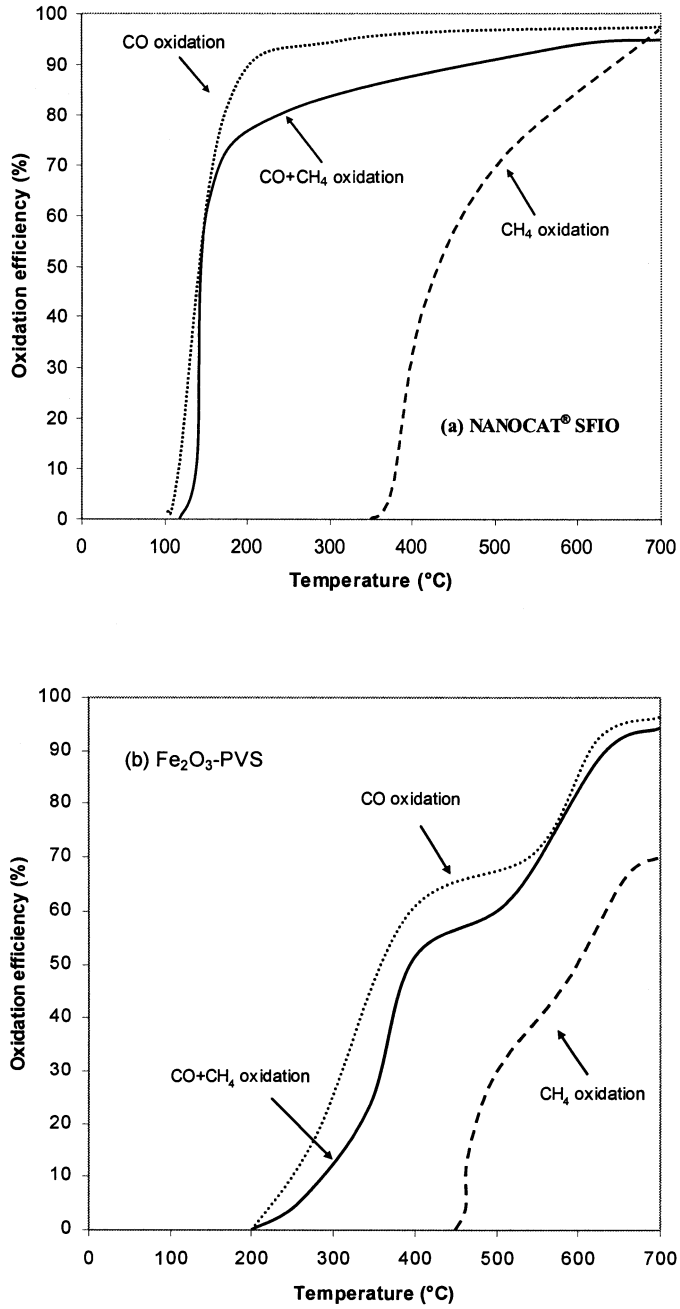

Figure 2.8. Efficiency of CO with CH_4 oxidation by NANOCAT® (a) and Fe_2O_3-PVS (b) as a function of temperature (Mass of NANOCAT®, 40mg; mass of Fe_2O_3-PVS, 400mg; flow rate of gas mixture, 55 cm^3/min; CO, 6.6%; CH_4, 1%; air, 92.4%).

4.3.2 Effect of concentration

The effect of inlet gas concentrations on the oxidation of CO with CH_4 to CO_2 by NANOCAT® and Fe_2O_3-PVS is shown in Figures 2.10a and 2.10b. The temperature and CO and CH_4 concentrations were varied, but the total flow rate was fixed at 55 cm^3/min. The results indicated that the lower concentrations of mixed inlet gas contributed to higher oxidation efficiency in the experimental range of temperatures. In Figure 2.10a, the oxidation efficiency over NANOCAT®, at the variable gas concentrations, improved sharply from 57.5% to 98.7% with increase in temperature for all inlet mix gas compositions except that in which 15% CO was mixed with 8.9% CH_4, whereas Figure 2.10b reveals a gradual increase in CO with CH_4 oxidation from 15% to 92% by Fe_2O_3-PVS.

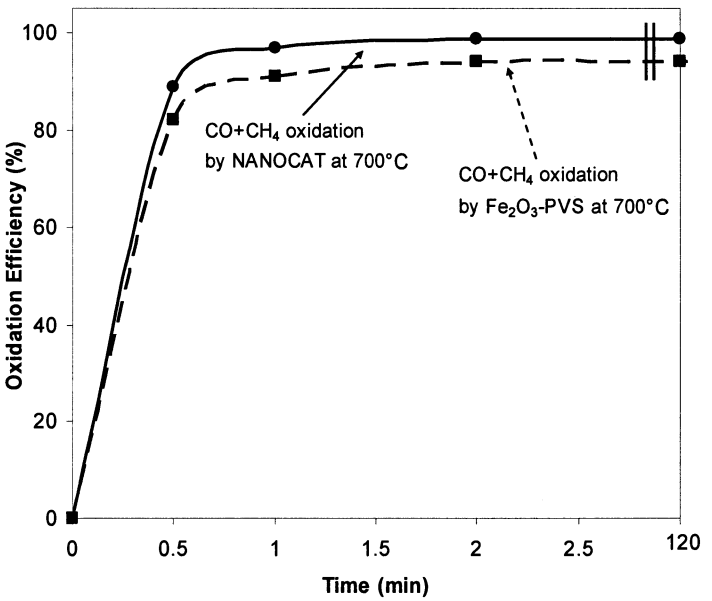

Figure 2.9. Efficiency of carbon monoxide mixed with methane oxidation during a period of 2 hours. (Mass of NANOCAT®, 40mg; mass of Fe_2O_3-PVS, 400mg; flow rate of gas mixture, 55 cm^3/min; CO, 6.6%; CH_4, 1%; air, 92.4%; temperature, 700 °C).

At a very high temperature of 700°C, the oxidation efficiency of a mixture of 15% CO and 8.9% CH_4 by the nanocatalyst improved only from 57.5 to 66.8% whereas by Fe_2O_3-PVS increased from 4.6% to 43.1%.

Insert Figures in Figure 2.10a and 2.10b recognize the concentration dependence of mixed gases at various temperatures. Total concentrations of mixed gas inlets are shown as the CO added to CH_4 percent. As shown in the figures, the increase of mixed gas concentration reduces the conversion efficiency of CO to CO_2 over the entire range of temperatures. The insert figure in Figure 2.10a demonstrates the NANOCAT® catalyzed oxidation of CO added to CH_4. The percentage of mixed gas oxidation is inversely dependent on its concentrations in the range of 300-700°C.

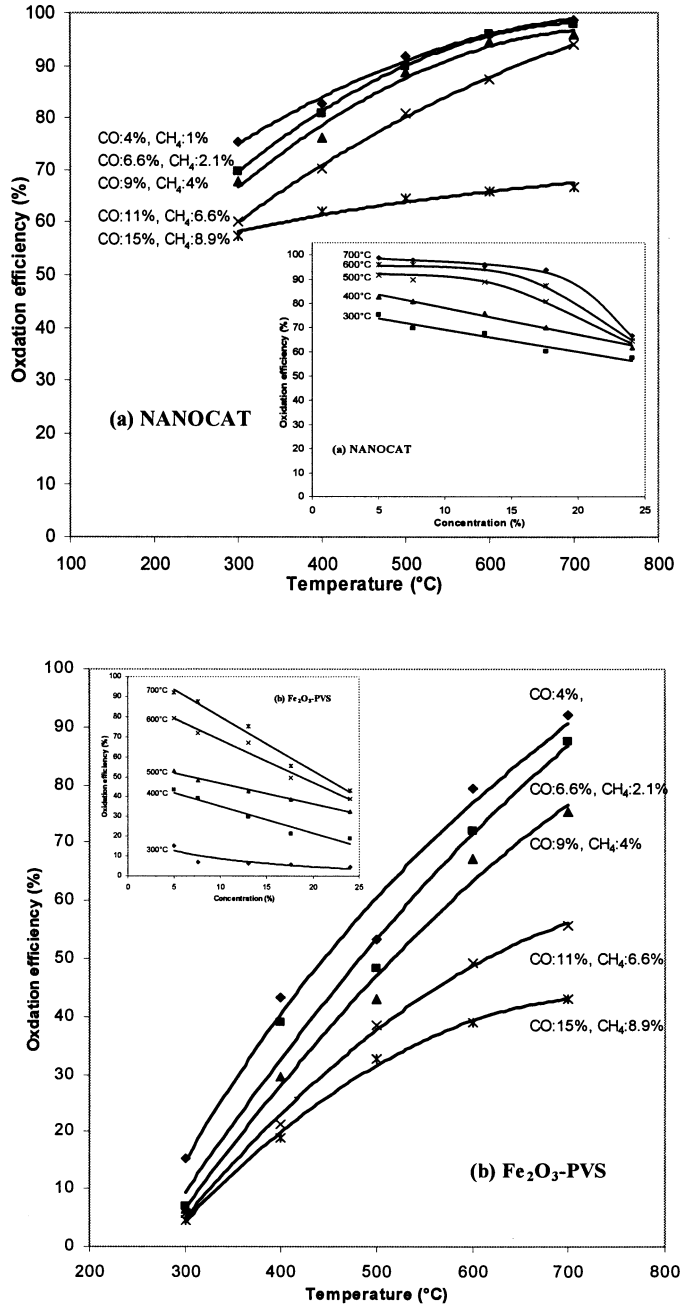

Figure 2.10. Efficiency of carbon monoxide with methane oxidation by NANOCAT® (a) and Fe_2O_3-PVS (b) at various concentrations; Insert Figures show oxidation efficiency as a function of the mixed gas concentration at various temperatures (Mass of NANOCAT®, 40mg; mass of Fe_2O_3-PVS, 400mg; flow rate of gas mixture, 55 cm^3/min).

A linear decrease of CO with CH_4 oxidation with increasing concentrations was noted at 300 and 400°C, whereas a sharp decrease was observed at a total 17% mixed gases between 500 and 700°C. Insert Figure 2.10b shows the linear decrease of oxidation by Fe_2O_3-PVS with the increase in inlet gas concentration. These results indicate that oxidation of CO mixed with CH_4 at high concentrations of mixed gas doesn't depend on the temperature, one of the critical factors, because of the difficulty of activating the CH_4.

4.3.3 Effect of space time

Experiments were performed at five different flow rates of inlet gas mixture at fixed 6.6% CO concentration and 1% CH_4 concentration for both NANOCAT® and Fe_2O_3-PVS. Figure 2.11 demonstrates the percentage of CO with CH_4 oxidation as a function of space time for the mixed gases and each catalyst at the various temperatures. Comparison of Figure 2.11a and 2.11b gives rise to the following observations: Figure 2.11a reveals no significant improvement of conversion efficiency by NANOCAT® with increasing the space time over the entire range of experimental temperatures. For the Fe_2O_3-PVS catalyst (Figure 2.11b), the oxidation improvement with increase in space time was minimal over the entire range of experimental temperatures. Moreover, oxidation efficiency by NANOCAT® (84.2%) was higher than that of Fe_2O_3-PVS (18.8%) at the lowest temperature of 300°C. These results suggest that the efficiency of mixed CO with CH_4 oxidation by NANOCAT® has little dependence on the space time and temperature, and the NANOCAT® catalyst itself rather than the conditions is the source of high oxidation rate.

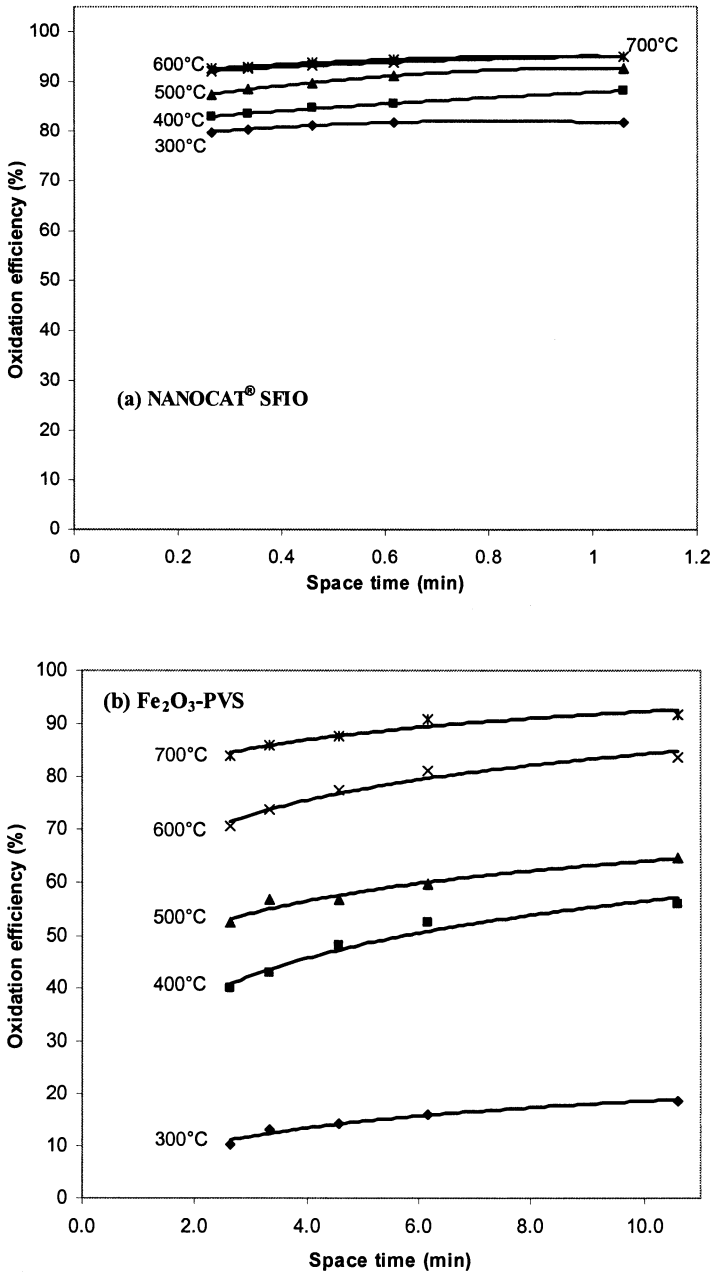

Figure 2.11. Efficiency of carbon monoxide with methane oxidation as a function of space time by NANOCAT®(a) and Fe_2O_3-PVS(b) (Mass of NANOCAT®, 40mg; mass of Fe_2O_3-PVS, 400mg; CO, 6.6%; CH_4, 1%; air, 92.4%).

CHAPTER 5. CONCLUSIONS

The catalytic oxidation of carbon monoxide and methane has been studied under various conditions of temperature, concentration and space time. On the basis of the catalytic activity results for NANOCAT® superfine Fe_2O_3 and Fe_2O_3-PVS as the oxidants, experimental results showed that these catalysts were highly efficient for oxidizing CO and CH_4, and mixtures of CO and CH_4; the oxidation product was CO and CO_2. Comparison of the effectiveness of NANOCAT® superfine Fe_2O_3 and Fe_2O_3-PVS catalysts indicates that the nanocatalyst (NANOCAT®) is more efficient for oxidizing CO, CH_4, and even mixtures of CO and CH_4 than Fe_2O_3-PVS, with CO_2 as the resulting product. The effectiveness of 40mg NANOCAT® for CO and CH_4 oxidation was higher than that of 400mg Fe_2O_3-PVS. Complete oxidation of CO was realized at relatively lower temperatures than was that of CH_4 oxidation, suggesting that the former is easier to activate than the latter. The higher activity of NANOCAT® over Fe_2O_3-PVS has been interpreted as being due to small particle size, high surface area, and denser surface coordination of the NANOCAT®. More research is needed to further explore the effectiveness of this promising catalyst, NANOCAT®, in the oxidation of other harmful gases such as SO_2 and other VOCs such as toluene and ethylene.

CHAPTER 6. REFERENCES

1. TimeDomain CVD, Inc. last visited April 30, 2005. http://www.timedomaincvd.com/CVD_Fundamentals/xprt/Plug_n_Pois.html
2. R. M. Heck, R. J. Farrauto, S. T. Gulati, Catalytic air pollution control, 2nd ed. WILEY-INTERSCIENCE (2002).
3. S. C. Kim, C. Y. Park, The complete oxidation of a volatile organic compound (toluene) over supported metal oxide catalysts. *Res. Chem. Intermed.* 28 (2002) 441–449.
4. H. Falcón, J. A. Barbero, G. Araujo, M. T. Casais, M. J. Martínez-Lope, J. A. Alonso and J. L. G. Fierro, Double perovskite oxides $A_2FeMoO_{6-\delta}$ (A=Ca, Sr and Ba) as catalysts for methane combustion. *Appl. Catal.* 53 (2004) 37-45
5. Heavy-Duty Diesel Emission Reduction Project Retrofit/Rebuild Component, EPA420- R- 99- 014 USA, (1999).
6. R. X. Zhou, X. Y. Jiang, J. X. Mao, X. M. Zheng, Oxidation of carbon monoxide catalyzed by copper-zirconium composite oxides. *Appl.Catal.* 162 (1997) 213-222.
7. P. Li, D. E. Miser, S. Rabiei, R.T. Yadav, M. R. Hajaligol, The removal of carbon monoxide by iron oxide nanoparticles. *Appl. Catal.* 43 (2003) 151-162.
8. J. Saint-Just, J. der Kinderen, Catalytic combustion: from reaction mechanism to commercial applications. *Catal. Today* 29 (1996) 387-395.
9. Yongjun He, Bolun Yang, Guangxu Cheng, Haimin Pan, Synthesis of $La_2O_3/BaCO_3$ nanocatalysts and their catalytic performance. *Powder Technol.* 134 (2003) 52– 57.
10. H. S Fogler, Elements of Chemical Reaction Engineering, 3rd Ed. Prentice Hall PTR (2000).

11. G. G. Hawley, The Condensed Chemical Dictionary, 9th ed. Van Nostrand Reinhold Co. (1977).

12. Carbon monoxide poisoning, last visited April 18, 2005. http://www.carbonmonoxidekills.com/

13. EPA- carbon monoxide, last visited April 18, 2005 http://www.epa.gov/iaq/co.html

14. J. T. Houghton, Climate Change. Cambridge University Press (1992).

15. M. Kang, M. W. Song, C. H. Lee, Catalytic carbon monoxide oxidation over CoOx/CeO2 composite catalysts. *Appl.Catal.* 251 (2003) 143-156.

16. H. Zhang, X. Hu, Catalytic oxidation of carbon monoxide in a fixed bed reactor. *Sep. Puri. Tech.* 34 (2004) 105-108.

17. EPA- methane, last visited April 18, 2005. EPA http://www.epa.gov/methane/

18. Chemical of the week- methane, last visited April 18, 2005. http://scifun.chem.wisc.edu/chemweek/methane/methane.html

19. Science Daily, last visited April 18, 2005. http://www.sciencedaily.com/

20. J.R. Paredes, S. Ordónez., A. Vega, F.V. Diýez, Catalytic combustion of methane over red mud-based catalysts. *Appl. Catal.* 47 (2000) 37–45.

21. Joo H. Lee, D. L. Trimm, Catalytic combustion of methane. *Fuel Prc. Technol.* 42 (1995) 339-359.

22. B. V. Reddy, F. Rasouli, M. R. Hajaligol, S. N. Khanna, Novel mechanism for oxidation of CO by Fe_2O_3 clusters. *Fuel* 83 (2004) 1537-1541.

23. Y.K. Rao, A physico-chemical model for reactions between particulate solids occurring through gaseous intermediates—I. Reduction of hematite by carbon. *Chem. Eng. Sci.* 29 (1974) 1435-1445.

24. N.R.E. Radwan, Modification of surfact and catalytic properties of Fe_2O_3 due to doping with rare-earth oxides Sm_2O_3 and Y_2O_3. *Appl. Catal.* 273 (2004) 21-33.

25. A.S.C. Brown, J.S.J. Hargreaves, B. Rijiniersce, The effect of sulfation on the activity of Fe_2O_3 catalysts for methane oxidation. *Topics in Catal.* 11/12 (2000) 181-184.

26. MACH I Inc., product bulletin (1999).

27. K. I. Choi, M. A. Vance, CO oxidation over Pd and Cu catalysts III. Reduced Al_2O_3-supported. *J. Catal.* 131 (1991) 1-21.

28. J. S. Walker, G. I. Straguzzi, W. H. Manogue, G. C. A Schuit, Carbon monoxide and propene oxidation by iron oxides for auto-emission control. *J. Catal.* 110 (1988) 299-313.

29. M. Haruta, S. Tsubota, T. Kobayashi, H. Kageyama, M. J. Genet, B. Delmon, Low-Temperature Oxidation of CO over Gold Supported on TiO_2, α-Fe_2O_3, and Co_3O_4. *J. Catal.* 144, (1993) 175-192.

30. M. M. Schubert, S. Hackenberg, A. C. Veen, M. Muhler, V. Plzak, R. J. Behm, CO Oxidation over Supported Gold Catalysts—"Inert" and "Active" Support Materials and Their Role for the Oxygen Supply during Reaction. *J. Catal.* 197 (2001) 113–122.

31. K.M. Bryden, K.W. Ragland, Numerical Modeling of a Deep, Fixed Bed Combustor, *Energy Fuels* 10 (1996) 269-275.

32. S. Minicò, S. Scirè , C. Crisafulli , R. Maggiore , S. Galvagno, Catalytic combustion of volatile organic compounds on gold/iron oxide catalysts. *Appl. Catal.* 28 (2000) 245-251.

33. S. Minicò, S. Scirè, C. Crisafulli, S. Galvagno, Influence of catalyst pretreatments on volatile organic compounds oxidation over gold/iron oxide. *Appl. Catal.* 34 (2001) 277-285.

34. S. Minicò, S.Scirè, C. Crisafulli, A.M.Visco, S.Galvagno, FT-IR study of Au/Fe2O3 catalysts forCO oxidation at low temperature. *Catal.Lett.* 47 (1997) 293-276.

35. P. Papaefthimiou, T. Ioannides, X. E. Verykios, VOC removal: investigation of ethylacetate oxidation over supported Pt catalysts. *Catal. Today* 54 (1999) 81–92.

36. N. Burgos, M. Paulis, M. M. Antxustegi, M. Montes, Deep oxidation of VOC mixtures with platinum supported on Al2O3/Al monoliths *Appl. Catal.* 38 (2002) 251–258.

37. E. Kullavanijaya, N. W. Cantl,D. L. Trimm, The treatment of binary VOC mixtures by adsorption and oxidation using activated carbon and a palladium catalyst. *J. Chem. Technol. Biotechnol.* 77 (2002) 473-480.

38. M. Kang, M. W. Song, C. H. Lee, Catalytic carbon monoxide oxidation over CoO*x*/CeO2 composite catalysts. *Appl.Catal.* 251 (2003) 143-156.

39. Bailey-PVS Oxides, L.L.C., last visited April 18, 2005 http://www.baileypvs.com/

40. J. M. Smith, Chemical Engineering Kinetics, 3rd ed. McGRAW-HILL BOOK COMPANY (1981).

41. W. Peukert, H. C. Schwarzer, F Stinger. Control of aggregation in production and handling of nanoparticles. *Chem. Eng. Process.* 44 (2004) 245-252

42. Joo H. Lee, D. L. Trimm, Catalytic combustion of methane. *Fuel Prc. Technol.* 42 (1995) 339-359

43. M. Lyubovsky, L. Pfefferle, Complete methane oxidation over Pd catalyst supported on a-alumina. Influence of temperature and oxygen pressure on the catalyst activity. *Catal. Today* 47 (1999) 29-44.